cytomety of MNC in the liver of mice treated with the IV injection of α-GalCer showed that the IFN-γ production of NKT cells in response to α-GalCer was suppressed by the treatment with adenosine and, consequently, the IFN-γ production of neutrophils that infiltrated the liver was also suppressed. Recently, Lappas et al. (*13*) reported that hepatic reperfusion injury was initiated by the activation of NKT cells that was inhibited by the adenosine A2A receptor agonist. Thus, these findings strongly suggest that the inhibitory effect of adenosine on prevention of early loss of transplanted islets is primarily mediated by NKT cells, although it remains uncertain whether the site of inhibitory action by adenosine includes the upstream pathway(s) of NKT cell activation, in which dendritic cells and macrophages (kupffer cells) might be involved.

Another important issue to consider is whether adenosine has protective effects directly on transplanted islets and whether islet cells express adenosine receptor(s). Recently, an adenosine receptor knockout mouse was developed (*26*), and it was reported that the tissue damage in Con A hepatitis was exacerbated in adenosine receptor $2A^{-/-}$ mice compared with wild-type mice (*27*). However, no information is available regarding whether islet cells themselves express adenosine receptors and whether adenosine has a direct protective effect on islet cells under stresses including hypoxia and inflammation. More importantly, the molecular mechanisms of the inhibitory effects by adenosine in the individual cells after binding adenosine receptor remain unclear. These issues are matters of interests for future investigations.

Because the low efficiency of islet transplantation remains a major obstacle to overcome in clinical islet transplantation, it is important and interesting to understand the extent and the efficiency of islet transplantation improvement by adenosine. The IPGTT at 60 days after transplantation disclosed that the glucose tolerance of STZ-induced diabetic mice receiving 200 islets from a single donor and treated with adenosine was superior in comparison with diabetic mice receiving 400 islets from two donors, thus indicating that adenosine facilitates a greater than 2-fold improvement in the efficiency of islet transplantation.

We found that the inhibitory effect of adenosine on the early loss of transplanted syngenic islets was also similar for islet allotransplantation, in which STZ-diabetic mice receiving 200 allogenic islets from a single donor and treated with adenosine became normoglycemic after the transplantation. However, the normoglycemic recipient mice became hyperglycemic again by 7 days after the transplantation, thus indicating that a single injection of adenosine has an inhibitory effect on the early loss of transplanted islets but not on the alloimmune rejection. Previously, we have shown that NKT cells play an essential role in alloimmune rejection of islet allografts in the liver of mice by using Vα14 NKT cell- and CD1d-deficient mice, in which the survival of islet allografts is prolonged without any immunosuppression (*28*). These findings suggest that adenosine may have an inhibitory effect on alloimmune rejection when administered appropriately with respect to its dosage and its duration, and with respect to the timing of the treatment. To clarify these, further studies are required. Importantly, a beneficial effect of adenosine on preventing the early loss of transplanted allogenic islets was found to be maintained when alloimmune rejection was prevented by anti-CD4 antibody. It is important to determine whether immunosuppressive agents such as antithymocyte globulin, which has been recently introduced into clinical islet transplantation, have any beneficial effect on the engraftment of transplanted islets. Furthermore, it is important to clarify whether the adenosine receptor agonist such as ATL-146e (*29*), which is currently being developed for clinical application, has any beneficial effect and how adenosine itself is effective in the improvement of the engraftment of transplanted islets in comparison to the other strategies including the procedures targeting proinflammatory cytokines (*19*) and instant blood-mediated inflammatory reactions (*30, 31*).

In summary, this study demonstrates that adenosine produces beneficial effects for the prevention of early loss of transplanted islets, enabling islet transplantation from one donor to one recipient in mice. Because adenosine and the adenosine transporter inhibitor, dipyridamole have already been used in the clinic, the safety issues with respect to the clinical use for islet transplantation has been cleared. Thus, adenosine may improve the efficiency of clinical islet transplantation provided that the beneficial effect of adenosine demonstrated in this study holds true in humans, although the effective dosage and the duration of the treatment still need to be clarified in a clinical setting.

ACKNOWLEDGMENT

The authors thank Dr. Masaru Taniguchi, RIKEN Research Center for Allergy and Immunology, Yokohama 230-0045, Japan, for providing α-galactocylceramide.

REFERENCES

1. Ricordi C, Strom TB. Clinical islet transplantation: Advances and immunological challenges. *Nat Rev Immunol* 2004; 4: 259.
2. Bellina MD, Kandaswamy R, Parkey J, et al. Prolonged insulin independence after islet allotransplants in recipients with type 1 diabetes. *Am J Transplant* 2008; 8: 2463.
3. Ryan EA, Lakey JRT, Rajotte RV, et al. Clinical outcomes and insulin secretion after islet transplantation with the Edmonton protocol. *Diabetes* 2001; 50: 710.
4. Drachenberg CB, Klassen DK, Weir MR, et al. Islet cell damage associated with tacrolimus and cyclosporine: Morphological features in pancreas allograft biopsies and clinical correlation. *Transplantation* 1999; 68: 396.
5. Fabian MC, Lakey JRT, Rajotte RV, r\et al. The efficiency and toxicity of rapamycin in murine islet transplantation. In vitro and in vivo studies. *Transplantation* 1993; 56: 1137.
6. Yasunami Y, Kojo S, Kitamura H, et al. Vα14 NKT cell-triggered IFN-γ production by $Gr\text{-}1^{+}CD11b^{+}$ cells mediates early graft loss of syngenic transplanted islets. *J Exp Med* 2005; 202: 913.
7. Fredholm BB, IJzerman AP, Jacobson KA, et al. International Union of Pharmacology. XXV. Nomenclature and classification of adenosine receptors. *Pharmacol Rev* 2001; 53: 527.
8. Haskó G, Pacher P. A_{2A} receptors in inflammation and injury: Lessons learned from transgenic animals. *J Leukoc Biol* 2008; 83: 447.
9. Németh ZH, Csóka B, Wilmanski J, et al. Adenosine A_{2A} receptor inactivation increase survival in polymicrobial sepsis. *J Immunol* 2006; 176: 5616.
10. Hoskin DW, Mader JS, Furlong SJ, et al. Inhibition of T cell and natural killer cell function by adenosine and its contribution to immune evasion by tumor cells [review]. *Int J Oncol* 2008; 32: 527.
11. Lappas CM, Rieger JM, Linden J. A_{2A} adenosine receptor induction inhibits IFN-γ production in murine $CD4^{+}$ T cells. *J Immunol* 2005; 174: 1073.

12. Deaglio S, Dwyer KM, Gao W, et al. Adenosine generation catalyzed by CD39 and CD73 expressed on regulatory T cells mediates immune suppression. *J Exp Med* 2007; 204: 1257.
13. Lappas CM, Day YJ, Marshall MA, et al. Adenosine A_{2A} receptor activation reduces hepatic ischemia injury by inhibiting CD1d-dependent NKT cell activation. *J Exp Med* 2005; 203: 2639.
14. Sutton R, McShane PM, Gray DWR, et al. Isolation of rat pancreatic islets by ductal injection of collagenase. *Transplantation* 1986; 42: 689.
15. Okeda T, Ono J, Takaki R, et al. Simple method for the collection of pancreatic islets by the use of Ficoll-Conray gradient. *Endocrinol Jpn* 1979; 26: 495.
16. Kemp CB, Knight MJ, Scharp DW, et al. Transplantation of isolated pancreatic islets into the portal vein of rats. *Nature* 1973; 244: 447.
17. Ohtsuka K, Yasunami Y, Ikehara Y, et al. Expansion of intermediate T cell receptor cells expressing IL-2R$\alpha^-\beta^+$, CD8$\alpha^+\beta^+$, and lymphocyte function-associated antigen-1^+ in the liver in association with intrahepatic islet xenograft rejection from rat to mouse: Prevention of rejection with anti-IL-2Rβ monoclonal antibody treatment. *Transplantation* 1997; 64: 633.
18. Watarai HR, Nakagawa M, Omori-Miyake N, et al. Methods for detection, isolation and culture of mouse and human invariant NKT cells. *Nature Protocol* 2008; 3: 70.
19. Satoh M, Yasunami Y, Matsuoka N, et al. Successful islet transplantation to two recipients from a single donor by targeting proinflammatory cytokines in mice. *Transplantation* 2007; 83: 1085.
20. Kawano T, Cui J, Koezuka Y, et al. CD1d-restricted and TCR-mediated activation of Vα14 NKT cells by glycosylceramides. *Science* 1997; 278: 1626.
21. Southard JH, Belzer FO. Organ preservation. *Ann Rev Med* 1995; 46: 235.
22. Ohta A, Sitkovsky M. Role of G-protein-coupled adenosine receptor in downregulation of inflammation and protection from tissue damage. *Nature* 2001; 414: 916.
23. Eltzschig HK, Abdulla P, Hoffman E, et al. HIF-1-dependent repression of equilibrative nucleoside transporter (ENT) in hypoxia. *J Exp Med* 2005; 202: 1493.
24. Resta R, Yamashita Y, Thompson LF. Ecto-enzyme and signaling functions of lymphocyte CD73. *Immunol Rev* 1998; 161: 95.
25. Desrosiers MD, Cembrola KM, Fakir MJ, et al. Adenosine deamination sustains dendritic cell activation in inflammation. *J Immunol* 2007; 179: 1884.
26. Ledent C, Vaugeois JM, Schiffmann SN, et al. Aggressiveness, hypoanalgesia and high blood pressure in mice lacking the adenosine A_{2a} receptor. *Nature* 1997; 388: 674.
27. Gomez G, Sitkovsky MV. Differential requirement for A2a and A3 adenosine receptors for the protective effect of inosine in vivo. *Blood* 2003; 102: 4472.
28. Toyofuku A, Yasunami Y, Nabeyama K, et al. Natural killer T-cells participate in rejection of islet allografts in the liver of mice. *Diabetes* 2006; 55: 34.
29. Rieger JM, Brown ML, Sullivan GW, et al. Design, synthesis, and evaluation of novel A2A adenosine receptor agonists. *J Med Chem* 2001; 44: 531.
30. Moberg L, Johansson H, Lukinius A, et al. Production of tissue factor by pancreatic islet cells as a trigger of detrimental thrombotic reactions in clinical islet transplantation. *Lancet* 2002; 360: 2039.
31. Ozmen L, Ekdahl KN, Elgue G, et al. Inhibition of thrombin abrogates the instant blood-mediated inflammatory reaction triggered by isolated human islets: Possible application of the thrombin inhibitor melagatran in clinical islet transplantation. *Diabetes* 2002; 51: 1779.

Diagnosis of Small Pancreatic Cancer by Endoscopic Balloon-Catheter Spot Pancreatography

An Analysis of 29 Patients

Seiyo Ikeda, MD, Kensei Maeshiro, MD,* Shinichiro Ryu, MD,* Kenji Ogata, MD,* Yohichi Yasunami, MD,* Yoshifuku Nakayama, MD,† and Yoshihiro Hamada, MD†*

Objectives: The diagnosis of small pancreatic cancer remains difficult. The present study describes the diagnostic value of endoscopic balloon-catheter spot pancreatography for small pancreatic cancer.

Methods: Since April 1984, balloon spot pancreatography has been used to detect small-sized pancreatic cancer in patients having possible symptoms or findings of obstructive pancreatitis.

Results: A resection was performed on 175 of 416 patients with conditions diagnosed as pancreatic cancer. Of the 175 patients, 23 (13%) had invasive carcinoma 2 cm or smaller based on histological measurements, 3 intraductal papillotubular adenocarcinoma, and 3 carcinoma in situ (CIS). Regarding invasive carcinoma, balloon pancreatography displayed duct abnormalities diagnosed as carcinoma in 20 of 22 patients, whereas carcinoma was suggested in 2. A definite diagnosis was obtained based on the findings of main duct stenosis or obstruction with marked stricture of the branch ducts (n = 18) and a filling defect in the main duct (n = 2). Moreover, this pancreatogram demonstrated an intraductal filling defect in 2 of 3 with intraductal carcinoma and dead twiglike findings in the branch ducts in 1 of 3 with CIS.

Conclusions: Balloon spot pancreatography is an essential tool for the diagnosis of small ductal pancreatic cancer, and it also makes it possible to locate CIS lesions of the branch ducts.

Key Words: small pancreatic cancer, balloon spot pancreatography, early diagnosis, invasive carcinoma ≤ 2.0 cm, carcinoma in situ

(*Pancreas* 2009;38: e102–e113)

Adenocarcinoma of the pancreas remains a highly lethal disease.[1–4] To improve the dismal outcome after a potentially curable resection, early diagnosis of this disease is required.[5–13] With recent advance in imaging studies such as computed tomography (CT), magnetic resonance imaging, endoscopic ultrasound (EUS), and positron emission tomography, a description of endoscopic retrograde cholangiopancreatography (ERCP) tends to no longer be included in papers on the diagnosis of pancreatic cancer. Can the diagnostic ERCP be ignored in the early diagnosis of pancreatic ductal cancer?

The authors[14] developed the technique of ERCP at the Cancer Institute Hospital, Tokyo, in 1968.[14,15] In the first paper on ERCP in 1970, Takagi et al[16] reported that the changes in the pancreatic duct system observed by pancreatography will contribute to the diagnosis of pancreatic tumors. However, contrary to expectations, no small pancreatic cancer has been detected by conventional endoscopic retrograde pancreatography (ERP) since then. In 1980, the case report of Takagi et al[17] about small pancreatic carcinoma in which an elevated urinary amylase level was found to be a clue for the diagnosis encouraged us to detect pancreatic cancer at an earlier stage.

Most pancreatic ductal cancer arises from the branch ducts.[18] This suggests that small pancreatic cancer could be detected if the fine branch ducts were more precisely visualized. Therefore, the endoscopic balloon-catheter spot pancreatography (balloon spot pancreatography) was developed in 1981.[19,20] To improve the diagnostic yield of ERP, 2 technical refinements were added: (1) removal of the endoscope while leaving the balloon catheter in the main pancreatic duct (MPD) to facilitate changing the position of the patient and (2) spot-film shooting with abdominal compression using a cone injecting the contrast medium in the supine position. These modifications of the ERP procedure permitted precise imaging of the MPD and fine branch ducts of the entire pancreas.[21] The diagnostic ability of conventional ERP was compared with that of this balloon method on resected cases. The rate of definite diagnosis increased from 71% to 97% and from 40% to 72% for pancreatic carcinoma and chronic pancreatitis, respectively, with the balloon pancreatography.[22] Trials are ongoing in which this method is used to diagnose small ductal cancer of the pancreas. The purposes of the present study were to demonstrate the high diagnostic value of balloon spot pancreatography for pancreatic small-sized cancer and to evaluate how this technique has contributed to an improvement of the surgical outcome.

MATERIALS AND METHODS

Balloon spot pancreatography was performed in 1012 patients from April 1984 to March 2005, including 300 patients with common-type pancreatic carcinoma, 382 patients with chronic pancreatitis, 172 patients with a cystic neoplasm such as intraductal papillary mucinous neoplasm (IPMN) and mucinous cystic neoplasm, and 158 patients with other conditions, including endocrine tumor of the pancreas, benign pancreatic cyst, and pancreaticobiliary maljunction. The success rate of this method was 97.8% (990/1012 patients). The number of balloon pancreatography procedures performed in 1012 patients was 1562. The complications associated with this procedure were acute pancreatitis in 30 patients, pseudocyst infection in 3, cholangitis in 3, and vasovagal reflex in 3. The total incidence was 2.5% (39 complications/1562 procedures), mostly acute pancreatitis with mild severity (1.9%).[22] No serious complications were encountered.

The balloon pancreatography method is diagramed in Figure 1. The procedure is similar to that of the standard ERP. A balloon catheter (350 cm long) is fully filled with a contrast medium (60% sodium diatrizoate) just before the insertion into

From the Departments of *Surgery and †Pathology, Faculty of Medicine, Fukuoka University, Fukuoka, Japan.

Received for publication September 13, 2008; accepted January 7, 2009.

Reprints: Seiyo Ikeda, MD, Department of Surgery, Faculty of Medicine, Fukuoka University, 7-45-1 Nanakuma, Johnan-ku, Fukuoka 814-0180, Japan (e-mail: s-ikeda@fukuoka-u.ac.jp).

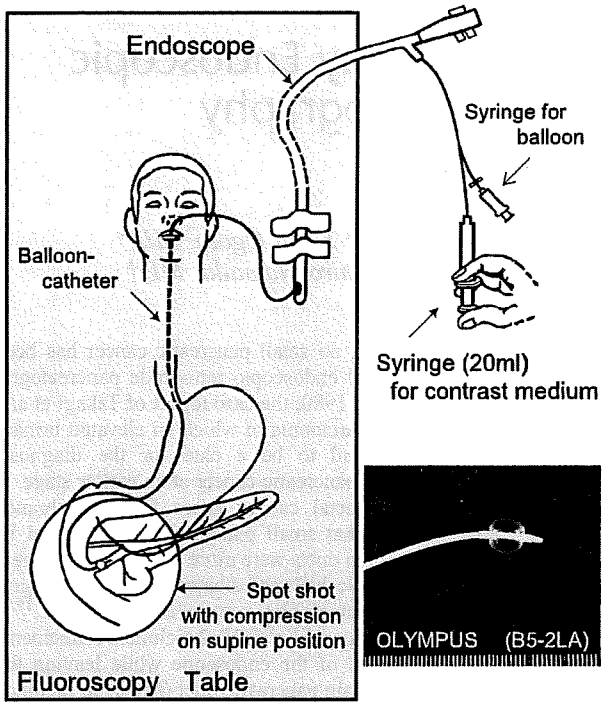

FIGURE 1. Procedure and devices used for endoscopic balloon-catheter spot pancreatography (balloon spot pancreatography).

the papilla orifice. At the same time, any air bubbles and even 1 drop of bile or duodenal juice present in the catheter tip must be flushed out. The balloon catheter is then cannulated into the pancreatic duct. A small amount of contrast medium is thereafter injected to fill the MPD. The balloon is inflated with air to keep the catheter tip in the duct and to prevent the contrast medium from flowing out. The endoscope is removed from the patient under fluoroscopy while leaving the catheter in place. The patient is then turned to the supine position. Abdominal compression spot shooting of the desired area is carried out, additionally injecting the contrast agent at a rate of approximately 1 mL/min (Fig. 1). This indwelling balloon method provided a complete and unobstructed view of the pancreatic ducts as the patient's posture can be easily changed under fluoroscopy.[21] Before deflation of the balloon, as much injected contrast medium as possible is usually retrieved with the syringe. This balloon method can usually be completed within 10 minutes.

Since April 1984, balloon spot pancreatography has been used to detect a small pancreatic cancer for patients having possible symptoms or findings of obstructive pancreatitis (Fig. 2).

Patients with IPMN and mucinous cystic neoplasms were excluded from this study. The whole resected specimen of the pancreas was examined using 5-mm stepwise tissue sections. The criteria for identifying pancreatic cancer measuring 2.0 cm or less in size (TS1) were based on histological 3-dimensional measurements. The tumor size presented in this paper shows the greatest dimension of an invasive area not including the length of intraductal spread from the main tumor.

RESULTS

Of 416 patients with conditions diagnosed as pancreatic cancer between April 1984 and March 2005, 175 had surgery with a curative intent (resection rate, 42.1%). Of the 175 patients, 23 (13%) had invasive carcinoma 2.0 cm or smaller, 3 had intraductal papillotubular adenocarcinoma, and 3 demonstrated carcinoma in situ (CIS; Table 1).

Clinical Characteristics

The clinical characteristics are described in Table 1. The clues to the diagnosis of the conditions of the 29 patients as TS1 cancer, intraductal papillotubular adenocarcinoma, and CIS were acute pancreatitis (10), upper abdominal pain (5), diabetes mellitus (DM; 3), checkup by US (3), hyperamylasemia (2), serum carbohydrate antigen (CA19-9; 1), and jaundice (5). A high level of amylase and/or elastase 1 was seen in 22 (76%) among the 29 patients.

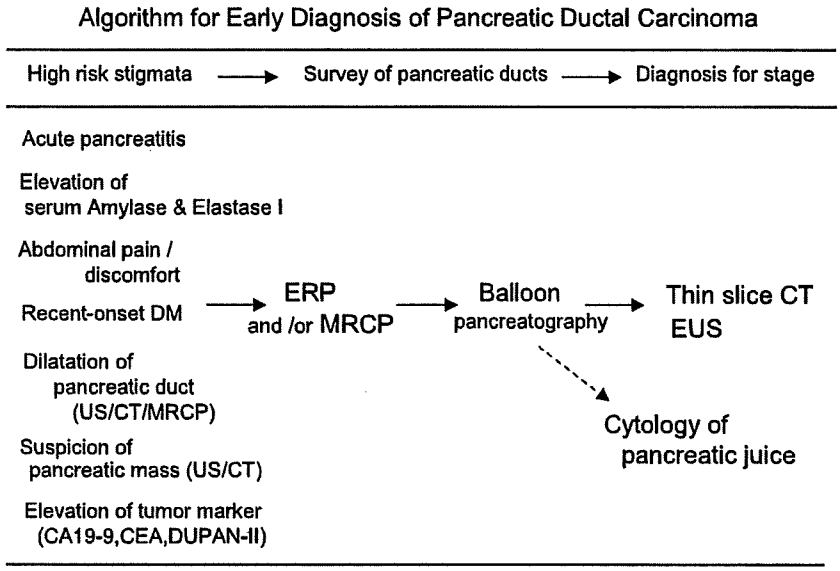

FIGURE 2. Diagnosis system of balloon spot pancreatography for high-risk patients.

TABLE 1. Characteristics of 29 Patients With Small Pancreatic Ductal Cancer

Patient No. Age/Sex	Clues to Diagnosis	Amy (50–160)	CA19-9 (437)	US/CT	ERP	Balloon pancreatography	Surgery	Tumor Size, mm	Histology	Stage* JPS[23]	Stage* UICC[46]	Outcome†
Invasive ductal carcinoma ≦ 2.0 cm: patient Nos. 1–23												
1) 57 M	Jaundice	WNL (Ela, 630)	62	Dilation of MPD	Occlusion of MPD	Filling defect in MPD	PD	13 × 10 × <13	Mod	III (CH+)	IA (T1 N0)	23 y 1 mo alive
2) 50 M	Acute pancreatitis‡	1,746	WNL	Mass?/cyst	Dilatation of BPD	Stenosis of BPD	PPPD	10 × 09 × 09 with ductal spread	Well	III (DU+)	IIA (T3)	6 y died
3) 74 F	Acute pancreatitis	650	67	Dilation of MPD	Occlusion of MPD	Stenosis of MPD·BPD	PPPD	20 × 20 × 13	Well	I (T1 N0)	IA	17 y 8 mo alive
4) 79 M	Jaundice	WNL	WNL	MPD dilation/ LDA(−)	Occlusion of MPD	Stenosis of MPD·BPD	PPPD	19 × 18 × 09	Mod	III (CH+)	IA	1 y 8 mo died
5) 72 F	Acute pancreatitis	3,130	55	Dilation of MPD	Stenosis of MPD	Stenosis of MPD·BPD	PPPD	20 × 19 × 18	Mod	I	IA	4 mo died
6) 53 M	Jaundice	WNL	WNL (Dup, 383)	Mass(−)/ LDA(−)	ERC only	Stenosis of BPD	PPPD	19 × 12 × 06	Mod	III (CH+ N1)	IIB (N1)	14 y 11 mo alive
7) 41 M	Jaundice	WNL (Ela, 450)	WNL (Dup, 5300)	Mass?/ LDA(−)	Occlusion of MPD	Stenosis of MPD·BPD	PPPD	18 × 15 × 13	Mod	III (CH+ N1)	IIB (N1)	3 y 4 mo died
8) 61 F	Jaundice	$103_{(20\text{-}80)}$ (Ela, 1290)	WNL (Dup, 5000)	Dilation of MPD	Occlusion of MPD	Stenosis of MPD·BPD	PPPD	15 × 12 × 11	Mod	III (CH+ N2)	IIB (N1)	13 y 4 mo alive
9) 72 M	Checkup (US)	242	WNL	Dilation of MPD	Occlusion of MPD	Stenosis of MPD·BPD	PPPD	08 × 06 × 04	Well	I	IA	7 y 3 mo alive
10) 63 F	Acute pancreatitis	2,749	48 (Dup, 392)	Dilation of MPD	Unsuccessful due to tumor		PPPD	20 × 16 × 15	Por	III (DU+ N1)	IIB (N1)	7 mo died
11) 66 M	Acute pancreatitis	869	WNL	Mass/LDA	Occlusion of MPD	Occlusion of MPD	PPPD	18 × 16 × 15	Well	III (N2)	IIB (N1)	1 y 7 mo died
12) 60 F	Amylase	442	WNL	Dilatation of MPD	Stenosis of MPD	Stenosis of MPD·BPD	PPPD	20 × 15 × 12	Por	III (CH+)	IA	6 y alive
13) 68 M	Epigastric pain	242	WNL (Dup, 230)	Dilatation of MPD	Occlusion of MPD	Occlusion of MPD	TP	15 × 14 × 13 with ductal spread	Por	I	IA	4 y 4 mo alive
14) 53 M	DM	WNL	WNL	Mass?/MPD dilation	Occlusion of MPD	Stenosis of MPD·BPD	DP	15 × 12 × 12	Mod	I	IA	15 y 9 mo alive
15) 67 M	Epigastric pain	WNL (Ela, 660)	WNL (Dup, 1600)	Mass/LDA	Occlusion of MPD	Occlusion of MPD	DP	16 × 15 × 09	Mod	IVb (T4 N2)	IV (M1)	3 mo died

16) 40 M	Epigastric pain	184	90 (Dup, 267)	Dilation of MPD	Occlusion of MPD	Stenosis of MPD·BPD	DP	15 × 13 × 12	Mod	III (N1)	IIB (N1)	10 mo died
17) 70 F	Upper abdominal pain	WNL	74	Mass/MPD dilation	Occlusion of MPD	Occlusion of MPD	DP	18 × 18 × 14	Mod	III (N1)	IIB (N1)	2 y 1 mo died
18) 51 F	Acute pancreatitis	618	86 (Dup, 176)	Mass/LDA	Occlusion of MPD	Occlusion of MPD	DP	19 × 18 × 17	Por	II (N1)	IIB (N1)	6 y 5 mo alive
19) 80 F	DM backache	WNL	41	Dilation of MPD	Occlusion of MPD	Occlusion of MPD	DP	16 × 09 × 05	Well	III (RP+)	IIA (T3)	1 y 8 mo died
20) 67 M	Amylase	172	WNL	Mass/MPD dilatation	Occlusion of MPD	Stenosis of MPD·BPD	DP	20 × 13 × 11	Mod	III (N1)	IIB (N1)	4 y 2 mo died
21) 54 F	Checkup (US)	WNL (Ela, 547)	WNL	Mass/HDA	Occlusion of MPD	Stenosis of MPD·BPD	PPPD	20 × 16 × 10	Well	II (N1)	IIB (N1)	5 y alive
22) 65 M	Checkup (US)	WNL	WNL	Mass?/LDA	Filling defect in MPD	Filling defect in MPD	DP	16 × 14 × 13	Well	I	IA	4 y 3 mo died
23) 70 M	Epigastric pain	WNL (Ela, 421)	WNL	Dilatation of MPD	Occlusion of MPD	Occlusion of MPD	DP	16 × 08 × 04	Por	I	IA	3 y 1 mo alive
Intraductal papillotubular adenocarcinoma with minute stromal invasion: patient Nos. 24–26												
24) 56 M	DM checkup	WNL (Ela, 470)	WNL	Dilatation of MPD	Filling defect in MPD	mass in MPD	PPPD		Pap	I	IA	11 y 7 mo alive
25) 48 M	Acute pancreatitis	996	WNL	Dilatation of MPD	Mass in MPD	mass in MPD	TP		Pap	I	IA	3 y 1 mo alive
26) 78 F	CA19-9	WNL	130	Blind spot/LDA	Occlusion of MPD	occlusion of MPD in tail	DP		Well	III (RP+)	IIA (T3)	3 y alive
CIS: patient Nos. 27–29												
27) 53 F	Acute pancreatitis	862	64	Dilatation of MPD	Occlusion of MPD	Stenosis of MPD	DP			CIS		15 y 7 mo alive
28) 62 F	Acute pancreatitis	2700	WNL (carcinoembryonic antigen, 8.7)	Mass(−)/ LDA(−)	Dilatation of BPD	Irregular stenosis of BPD	PPPD			CIS		4 y died
29) 58 F	Acute pancreatitis	2650	WNL	Mass(−)/ MPD Dilatation	Stenosis of MPD	Stenosis of MPD	MP			CIS		3 y 2 mo alive

*Staging according to the classification of the JPS second English edition[23] and the UICC sixth edition.[46]

†Outcome in March 2008.

‡Acute pancreatitis was defined as abdominal pain with high level more than 3 times of normal value of serum amylase.

Amy indicates amylase; WNL, normal; Dup, dupan2; Ela, elastase I; CH+, distal bile duct invasion; DU+, duodenal invasion; RP+, retropancreatic invasion; BPD, branch pancreatic duct; DP, distal pancreatectomy; TP, total pancreatectomy; Mod, moderately differentiated type; MP, middle pancreatectomy; Por, poorly differentiated type; Well, well differentiated type.

Invasive Ductal Carcinoma (TS1): Patient Nos. 1 to 23

Conventional ERP and balloon spot pancreatography were successful in 21 and 22 patients, respectively. In patient No. 10, both the procedures ended in failure because the tumor was located near the orifice of the MPD. The findings of the MPD obstruction by ERP were converted into those of the MPD stenosis by balloon spot pancreatography in 9 patients, leading to precise visualization of the severe branch duct stricture in the area of the MPD stenosis (Figs. 4A, B). As a result, those findings of the branch ducts displayed by the balloon method were very useful in differentiating pancreatic cancer from chronic pancreatitis.

Balloon spot pancreatography demonstrated duct abnormalities that were diagnosed to be carcinoma in 20 (91%) of 22 patients and were suggestive of carcinoma in another 2 (9%). The findings of the former were localized stenosis of the MPD with marked stricture of the surrounding branch ducts (n = 11), a complete tapered obstruction of the MPD (n = 7), and a filling defect in the MPD (n = 2). Those of the latter were only regional stenosis of the branch duct (n = 2), which was not visualized by conventional ERP. On the other hand, post–contrast CT scan revealed a low-density area, suggesting cancer only in 4 of the 23 patients (17%), but it showed a dilatation of the MPD (n = 14) and the branch duct (n = 1) in 15 of the remaining 19.

The tumor was located in the head of the gland in 13 patients and in the body and tail in 10. The surgical procedures included pylorus-preserving pancreatoduodenectomies (PPPDs, n = 12), a pancreatoduodenectomy (n = 1), a total pancreatectomy (n = 1), and distal pancreatectomies (n = 9). All patients underwent a regional lymphadenectomy (D2 of Japan Pancreas Society [JPS] rule[23]). Adjuvant chemotherapy was given to 8 patients (patient Nos. 1, 6, 10, 13–15, 19, and 22).

A histological examination demonstrated invasive ductal carcinoma of the well-differentiated type in 7, moderately differentiated type in 11, and poorly differentiated type in 5. Of the 23 patients, 11 (48%) had lymph node metastases; 7 patients were in stage I, 2 in stage II, 13 in stage III, and 1 in stage IVb according to the JPS classification[23] (Table 1).

None of the 23 patients were lost during the long-term follow-up. In 20 patients, whose resection for pancreatic cancer was performed more than 5 years ago, 10 passed the 5-year survival line, for an actual 5-year survival rate of 50%. One patient died at 6 years of a local recurrence. Nine patients remain well without evidence of recurrence as of March 31, 2008. Five of them have survived more than 10 years (range, 13–23 years).

Representative Cases of TS1 Carcinoma (Cases 1 to 3)

Case 1: A Clue for the Diagnosis—The Onset of Acute Pancreatitis (Patient No. 3)

A 74-year-old woman developed acute severe pancreatitis with shock. Abdominal US and CT scan (Fig. 3A) showed dilatation of the MPD. After her general conditions improved, she underwent conventional ERP. The ERP had the findings suggestive of pancreas divisum (Fig. 3B). Thereafter, she was referred for further examination. Her serum CA19-9 (<37) level was 67. Balloon spot pancreatography demonstrated a marked stenosis of the MPD and a masslike shadow in the dilated duct during the abdominal compression stage of this procedure (Fig. 3C). A PPPD with a regional lymphadenectomy was performed. The pancreatic head tumor was limited to the pancreas (Fig. 3D). Histologically, the tumor was an invasive ductal carcinoma, measuring 20 × 20 × 13 mm in dimension and close to the strictured duct (Fig. 3E). The masslike filling defect in the dilated duct was because of a papillary lesion, histologically diagnosed as atypical hyperplasia (Fig. 3F). She is doing very well without any signs of cancer recurrence 17 years after the operation.

Case 2: A Clue for the Diagnosis—Diabetes (Patient No. 14)

A 53-year-old man received a medical checkup, and his condition was diagnosed as DM. Four months later, US and CT scan showed dilatation of the MPD. Endoscopic retrograde pancreatography disclosed a tapered obstruction of the MPD (Fig. 4A). Balloon spot pancreatography clearly visualized a severe localized stenosis of the MPD accompanied by highly stenotic branch ducts thus causing a gap (Fig. 4B, yellow arrow). A distal pancreatectomy and splenectomy were then performed with a lymph node dissection of D2.[23] The cut surface of the specimen disclosed a strictured MPD (Fig. 4C). A histological examination revealed invasive ductal carcinoma of the moderately differentiated type, measuring 15 × 12 × 12 mm (Figs. 4D, E). The patient is now doing very well at 15 years 9 months after surgery.

Case 3: A Clue for the Diagnosis—Hyperamylasemia (Patient No. 12)

A 60-year-old woman was admitted for the treatment of pneumonia. She underwent US, CT scanning, and magnetic resonance cholangiopancreatography (MRCP) because of an elevation of her serum amylase level (442 IU/L). Ultrasound showed a cyst in the pancreatic head (Fig. 5A). Computed tomographic and MRCP images disclosed a diffuse dilated MPD with cystic lesions (Figs. 5B, C). Conventional ERP demonstrated a smooth narrowing of the MPD and branch ducts (Fig. 5D). Balloon spot pancreatography precisely visualized the marked stenosis of the MPD and branch ducts, thus leading to the diagnosis of small pancreatic carcinoma (Fig. 5E). A small hypoechoic mass was confirmed in the area by EUS (Fig. 5F). A PPPD with D2 lymph node dissection[23] was performed. Macroscopically, the resected specimen showed a 15-mm-diameter tumor in the area corresponding to the stenosis of the MPD (Fig. 5G). A microscopic examination revealed the tumor to consist of a poorly differentiated adenocarcinoma, infiltrating into the lower bile duct wall (Figs. 5H, I). She has shown a disease-free survival of 6 years after the operation.

Intraductal Papillotubular Adenocarcinoma With Minute Stromal Invasion: Patient Nos. 24 to 26

Balloon spot pancreatography disclosed a masslike filling defect in the MPD diagnosed as intraductal carcinoma in patient Nos. 24 and 25 and a tapered obstruction of the MPD suggestive of small invasive cancer in patient No. 26. A total pancreatectomy in patient No. 25 was performed because an intraoperative histological examination showed a widely intraductal spread of cancer. These 3 cases were classified as intraductal papillotubular adenocarcinomas, not IPMN based on the patterns of mucin expression.[24]

Representative Case of Intraductal Adenocarcinoma (Case 4)

Case 4: A Clue for the Diagnosis—Diabetes (Patient No. 24)

A 56-year-old man had a medical checkup, resulting in the diagnosis of DM. Ultrasound and CT scan showed dilatation of the MPD. Endoscopic retrograde pancreatography

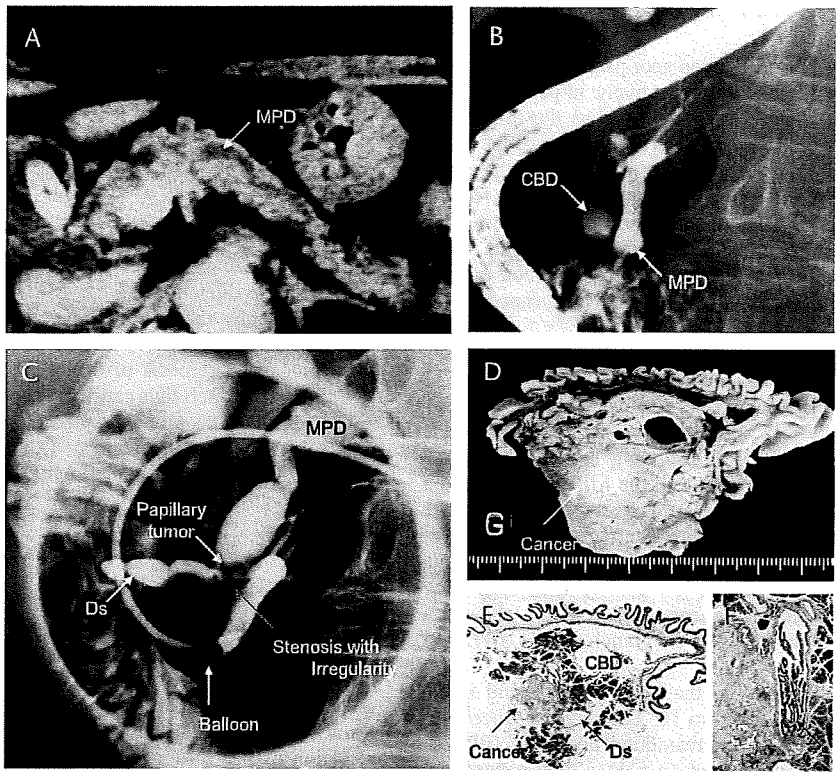

FIGURE 3. Case 1. A, Dilatation of the MPD (CT). B, No visualization of the distal pancreatic duct (ERP). C, Marked irregular stenosis of the MPD and a masslike lesion in the dilated duct (balloon spot pancreatography). D, A solid mass (cancer) in the head of the pancreas. E, Loupe of the representative section; CBD, common bile duct; Ds, Santorini duct. F, Papillary atypical epithelium highly suggestive of malignancy in the MPD.

outlined a vague small filling defect in the MPD. Balloon spot pancreatography displayed an intraductal mass in the MPD (Fig. 6A). A PPPD with regional lymph node dissection was performed. The macroscopic findings showed the polypoid tumor arising in the dilated subbranch and protruding into the lumen of the MPD (Figs. 6B, C). Microscopically, the carcinoma was mostly confined within the duct but had invaded the surrounding stroma with a tubular infiltrating pattern (Fig. 6D). He is doing well 11 years after the PPPD.

Carcinoma In Situ: Patient Nos. 27 to 29

The presence of acute pancreatitis was a clue for the diagnosis of CIS in these 3 cases. Balloon spot pancreatography demonstrated regional stenosis of the MPD in patient Nos. 27 and 29 and the irregular width and narrowness of the branch ducts in patient No. 28, which were suggestive of cancer. In the 2 patients with the stenotic MPD, the histological examination of a frozen section showed CIS.

Representative Case of CIS (Case 5)

Case 5: A Clue for the Diagnosis—Acute Recurrent Pancreatitis (Patient No. 28)

A 62-year-old woman had developed acute pancreatitis several times since 1995. Serum carcinoembryonic antigen (normal ≤ 5.0) showed 8.7 ng/mL. Ultrasound and CT scans displayed no abnormal findings. Endoscopic retrograde pancreatography demonstrated a small cystic dilatation of the branch ducts (Fig. 7A). Pancreatic juice cytology revealed class IV suggestive of cancer. Balloon spot pancreatography disclosed findings of dead twiglike branch ducts (Figs. 7B, C), resulting in localizing the intraductal epithelial lesions. A PPPD with lymph node dissection[23] of D2 was performed. The cut surface of the specimen showed whitish inflammatory changes adjacent to the cystic dilatation of the branch duct (Fig. 7D). A histological examination represented highly atypical duct epithelium equivalent to CIS (Figs. 7E, F). Immunohistochemistry demonstrated that p53 tumor suppressor gene product was shown to be overexpressed in the epithelial lesions (Fig. 7G). Three years after the PPPD, locoregional recurrence occurred. Although an en bloc resection of the recurrence site was attempted, it ended in a partial resection of the pancreas and the invasive retroperitoneal tumor. Histologically, CIS of the MPD was seen, but no other invasive carcinoma was identified in the pancreatic parenchyma. The retroperitoneal tumor presented a pattern of perineural invasion. Therefore, a possible cause of the local recurrence could be explained by (1) a frozen section of the MPD margin of the resected pancreas was diagnosed as having slightly atypical epithelial cells. However, a highly atypical epithelium (Figs. 7H, I) of the MPD was revealed by the histological reexamination of the pancreatic neck margin of the initial resection at the time that the local recurrence appeared. Therefore, the CIS left in the MPD near the stoma invaded retroperitoneally. (2) Another would be that floating cancer cells in the pancreatic juice that leaked from the anastomotic site implanted. The patient died 1 year after the second operation.

DISCUSSION

The early diagnosis of pancreatic ductal adenocarcinoma is indispensable to achieve a better surgical outcome.[5–13] Despite recent advances in imaging modalities, however, there are still few reports of small common-type pancreatic cancer 2 cm or smaller. This paper demonstrated that ERP followed by balloon spot pancreatography was very useful for the diagnosis of TS1 cancer defined by strict histological measurements. The precise duct abnormalities of the MPD and branch ducts in the 22 patients visualized by the balloon pancreatography contributed to the diagnosis of TS1 cancer. The findings by balloon spot pancreatography to differentiate pancreatic invasive cancer from chronic pancreatitis were specifically the marked stricture of the MPD with a gap or irregular stenosis of the branch duct. The balloon method is superior in its diagnostic capability to the standard ERP because of greater yields from the pancreatogram. On the other hand, post–contrast CT scans presented low-density areas characteristic of cancer only in 4 (17%) of the 23 patients. Consequently, the low diagnostic sensitivity of CT scanning for pancreatic TS1 cancer suggests that the presence of a pancreatic cancer should not be ruled out based on conventional CT scanning. Ishikawa et al[9] also described that duct dilatation alone depicted by US/CT should not be overlooked because of the low diagnostic sensitivity (26%) of CT scanning for cancers of 1.0 cm or less. Endoscopic US has increasingly been used in the diagnosis and staging of pancreatic malignancies. However, EUS is limited by its inability to differentiate between malignant and inflammatory pancreatic lesions.[25,26] In fact, the smallest cancer (8 × 6 × 4 mm) with surrounding fibrosis in patient No. 9 was diagnosed as having a cancer measuring 26 × 22 mm by EUS (not shown). Furthermore, CIS cannot be diagnosed with EUS. Owing to the previously mentioned findings, CT scanning and EUS are performed after balloon pancreatography in the current diagnostic algorithm for pancreatic ductal carcinoma. The reason why ERP and/or MRCP are performed as the initial step is to identify the region that need to be scanned by balloon spot pancreatography (Fig. 2).

Acute pancreatitis, high level of serum pancreatic enzyme,[27] recent-onset DM,[28–31] and indirect findings such as dilated pancreatic ducts[32,33] and cystic lesions by US, MRCP, or CT scan must all be addressed as possible indications of pancreatic carcinoma. Of the 29 patients with small pancreatic carcinoma, 10 (34%) had acute pancreatitis as a clue to the diagnosis. Among them, there was 1 patient with TS1 cancer who had only a marked stricture of the branch duct.[34] Moreover, high level of serum amylase and/or elastase 1 was seen in 76% of the 29 patients. Therefore, small pancreatic cancer could be detected if more patients at high risk for pancreatic cancer were scanned with this diagnostic system. Acute pancreatitis can be caused by obstruction of the draining ducts by intraductal epithelial lesions.[35] The current study described 3 cases of histologically proven CIS of the pancreas in which the presence of acute

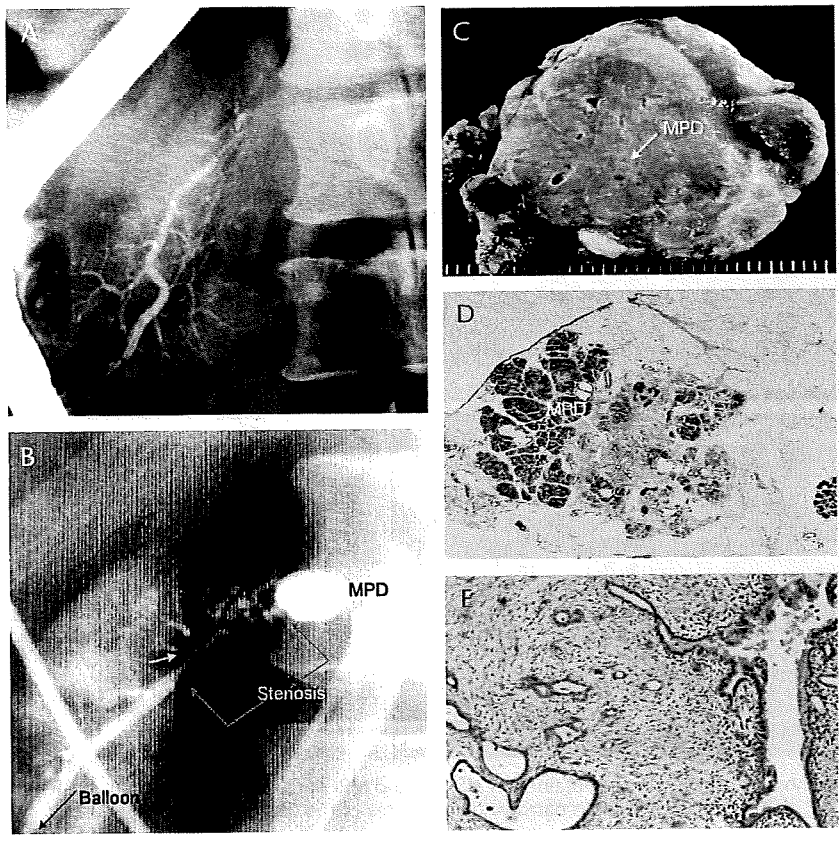

FIGURE 4. Case 2. A, A tapering obstruction of the MPD (ERP). B, A severe localized stenosis of the MPD in the body. No branch duct visualized below the stenosis (red arrow) and highly stenotic branch ducts showing a gap (small arrow; balloon spot pancreatography). C, Marked stricture of the MPD (arrow). D and E, Moderately differentiated tubular adenocarcinoma.

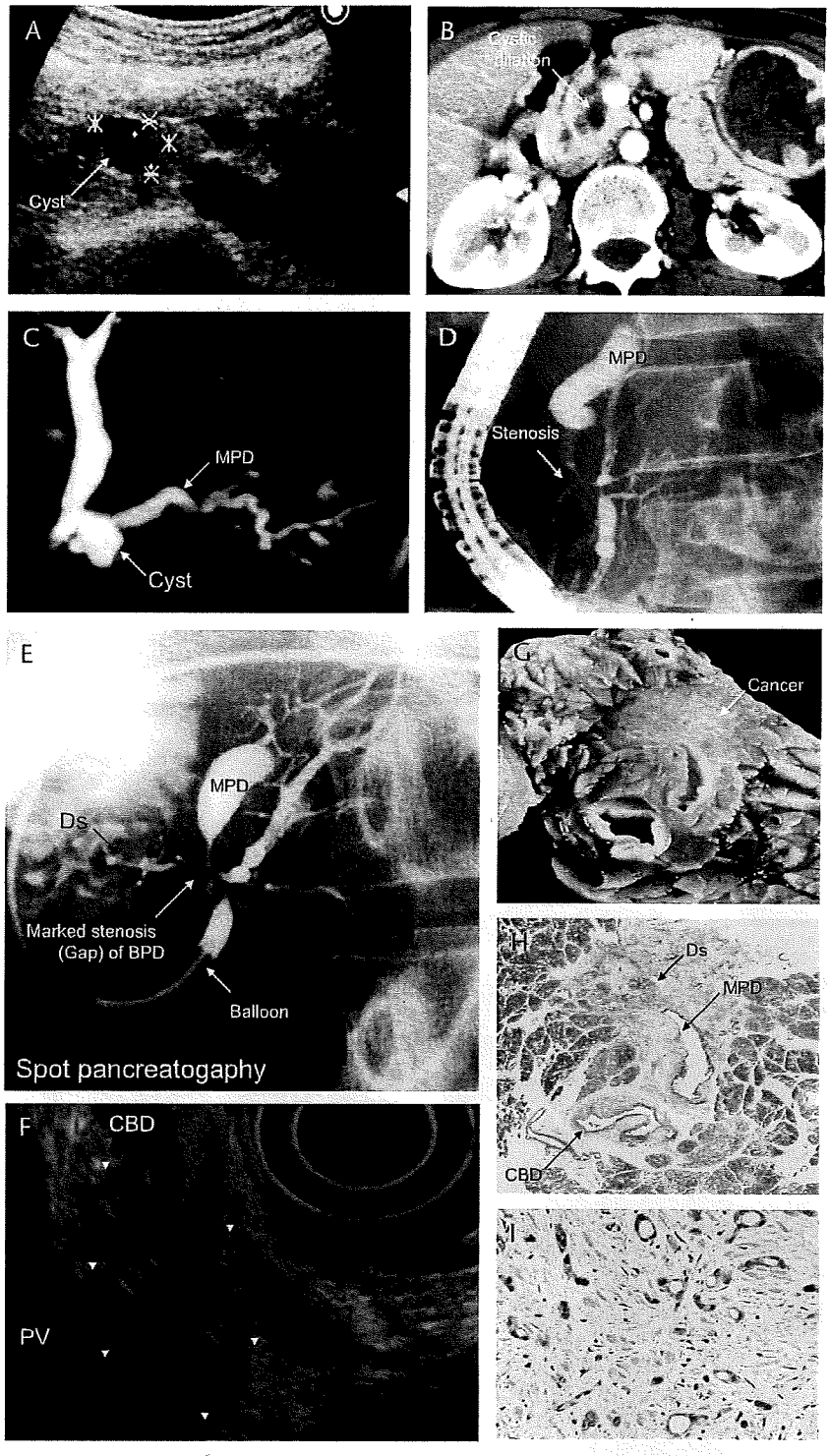

FIGURE 5. Case 3. A–D, Diagnosis of cancer was not obtained by US, CT, and MRCP. (A–C) Cystic dilatation of the pancreatic duct in the head of the pancreas (US, CT, and MRCP). (D) Smooth narrowing at the area of the confluence of the MPD and Santorini duct highly suggestive of carcinoma (ERP). E–I, Balloon spot pancreatography displayed findings characteristic of cancer. (E) Severe stenosis at the area of the junction between the MPD and Santorini duct. Marked stricture of the branch ducts showing gap (arrow) that is useful in differentiating cancer from chronic pancreatitis (balloon spot pancreatography). (F) An ill-defined hypoechoic mass with an irregular echogenicity (EUS). (G) A solid whitish mass in the head of the pancreas. (H and I) Poorly differentiated adenocarcinoma

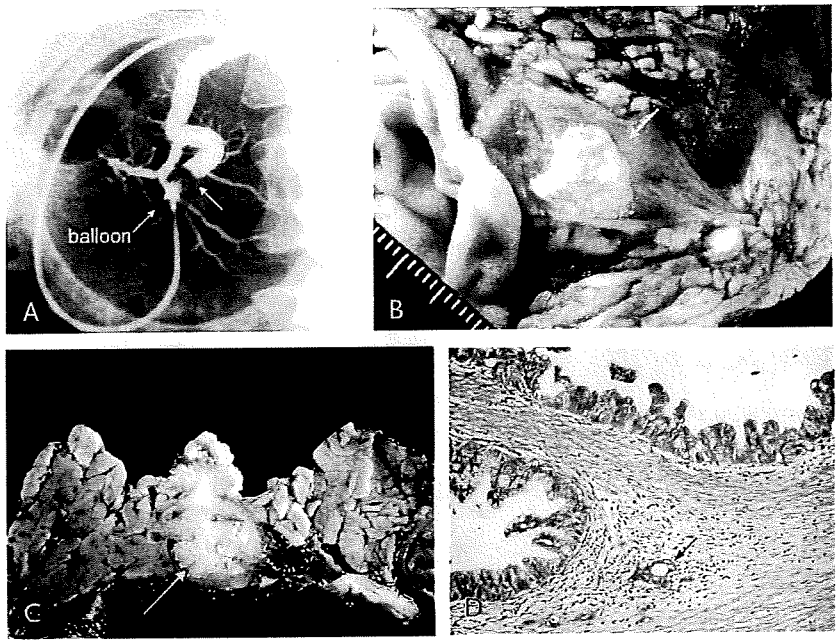

FIGURE 6. Case 4. A, Tumor in the MPD visualized by abdominal compression (balloon spot pancreatography). B, Polypoid tumor protruding into the lumen of Wirsung duct (arrow). C, Papillary tumor mainly occupied in the branch duct (arrow). D, Minute tubular stromal invasion (arrow).

pancreatitis was a clue for the diagnosis. Endoscopic retrograde pancreatography showed segmental narrowing of the MPD in 2 of those cases and only small cystic dilatation of the branch duct in the pancreatic head in 1. In the latter case, where the pancreatic juice cytology was class IV, balloon spot pancreatography demonstrated dead twiglike findings of irregular width and narrowness in the some branch ducts adjacent to the small cyst as shown in Figure 7A. Therefore, it was possible to locate the intraductal lesions in the head of the pancreas, and a PPPD was performed. However, locoregional recurrence developed 3 years later. This case suggested that an accurate frozen section diagnosis for atypical grade[36–40] of the duct epithelium was indispensable to prevent leaving CIS in the remaining MPD.

Endoscopic retrograde cholangiopancreatography is generally considered to be an invasive diagnostic tool that may cause post-ERCP severe acute pancreatitis.[41,42] Endoscopic retrograde cholangiopancreatographies have been performed in 400 to 600 patients per year in the Fukuoka University Hospital since April 1984, and no incidence of serious post-ERCP pancreatitis has been experienced without the use of any prophylactic drugs.[15] The ERCP-induced pancreatitis tends to occur more after a procedure of endoscopic retrograde cholangiography (ERC) intent than that of ERP. The time required for ERP is only 5 to 10 minutes because the cannulation of ERP is usually easier in comparison to the ERC, which required inserting a catheter further upward. Therefore, it is advisable to review ERP and ERC individually about the postprocedure complications of ERCP.

The authors previously performed cholangiography[43–45] of the intrahepatic bile ducts in cases of hepatolithiasis by the endoscopic placement of an indwelling balloon catheter at Kyushu University Hospital before the development of balloon spot pancreatography. Therefore, the application to ERP of this indwelling balloon-catheter ERC was developed leading to the design of a device for balloon spot pancreatography. Initially, there was concern that post-ERP pancreatitis would develop because of the increased intraductal pressure caused by the balloon block. However, none of the first 48 patients who underwent balloon pancreatography using an infusion pump developed acute pancreatitis.[20] So far, the procedures have been performed more than 1500 times in this hospital with a low incidence of post–balloon pancreatography pancreatitis.[22] The authors believe that the most important point for preventing post-ERP pancreatitis is not to inject even 1 drop of bile or duodenal juice that could activate pancreatic enzymes in the pancreatic duct, thus causing acute pancreatitis. Again, the importance of inserting a catheter into the orifice of the duodenal papilla while letting a contrast medium flow out of the catheter tip is emphasized. A syringe of 20 mL is necessary to make a sufficient contrast material spout out to expel any air bubbles, bile, or duodenal juice that might be present in the catheter tip.[15]

The current series reflects the experience at Fukuoka University Hospital. There are no reports of TS1 pancreatic cancer defined with strict criteria based on histological 3-dimensional measurements. Consequently, the results presented herein might express the actual situation regarding the diagnosis, stage, and surgical late outcome in TS1 pancreatic cancer. Ten of 20 patients survived more than 5 years after surgery. Therefore, the actual 5-year survival rate without any statistical manipulation was 50%. It is not rare to observe late recurrence for 5 years after surgery in pancreatic cancer,[1] whereas 9 of the 10 patients are currently alive without a sign of recurrence. In addition, 5 patients have also survived well for 10 years.

Considering that most pancreatic ductal cancer originates from the branch duct,[18] invasive cancer forming a mass can easily infiltrate beyond the flat pancreas. Therefore, CIS or minimally invasive ductal carcinoma must be detected to improve the surgical results.[8,11] Such early ductal cancer cannot

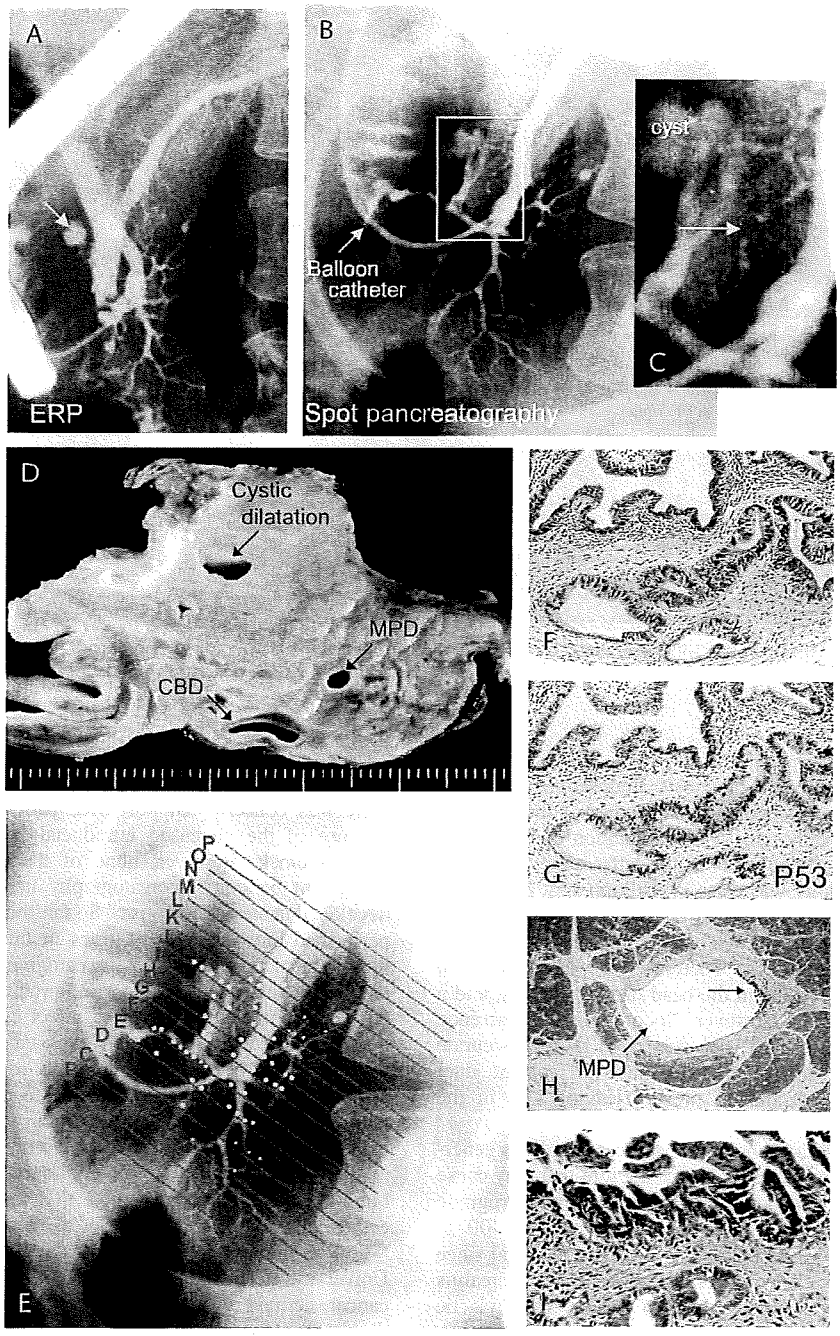

FIGURE 7. Case 5. A–C, Duct abnormalities of the branch ducts visualized by ERP and balloon spot pancreatography. (A) Small cystic dilatation of the branch ducts (arrow, ERP). (B) Dead twiglike findings of the branch ducts in a rectangular line (balloon spot pancreatography). (C) Irregular width and narrowness of those ducts disclosed by the magnified image (arrow). D–I, Macroscopic and histological findings. (D) Whitish inflammatory changes around the cystic branch duct. (E) The widely intraductal spread of in situ carcinoma shown with yellow spots. (F) The CIS of the branch duct near the cystic duct. (G) P53 overexpressed in the high-grade duct lesion. (H) The MPD near the pancreatic margin in the resected specimen from the primary operation. Atypical duct lesions (arrow) found in the MPD epithelium that avoided desquamation. (I) The CIS seen in the MPD epithelium.

normally be diagnosed by imaging modalities that are used to identify the presence of an invasive intraparenchymal mass. The diagnostic procedures for pancreatic ductal carcinoma should be carried out using precise pancreatograms and thus facilitating further examinations, such as cytology or molecular biological assays of pancreatic juice specimens.

ACKNOWLEDGMENTS

The authors thank Dr Kunio Takagi, former vice-director of the Department of Surgery, Cancer Institute Hospital Tokyo for his continuous encouragement and Dr Hidenobu Watanabe, Professor Emeritus, Niigata University for his helpful comments about histopathological analyses. The authors are grateful to Dr Masao Tanaka, Professor, Department of Surgery and Oncology, Graduate School of Medical Sciences, Kyushu University for giving helpful advice. The authors are also indebted to the staff of the Department of Surgery, Radiology and Pathology, Faculty of Medicine, Fukuoka University for their clinical and pathological supports.

REFERENCES

1. Trede M, Schwall G, Saeger H. Survival after pancreatoduodenectomy: 118 consecutive resections without an operative mortality. *Ann Surg.* 1990;211:447–458.
2. Cameron JL, Crist DW, Sitzmann JV, et al. Factors influencing survival after pancreaticoduodenectomy for pancreatic cancer. *Am J Surg.* 1991;161:120–125.
3. Conlon KC, Kimstra DS, Brennan MF. Long-term survival after curative resection for pancreatic ductal adenocarcinoma: clinicopathologic analysis of 5-year survivors. *Ann Surg.* 1996;223:273–279.
4. Matsuno S, Egawa S, Furuyama S, et al. Pancreatic cancer registry in Japan: 20-years experience. *Pancreas.* 2004;28:219–230.
5. Tsuchiya R, Noda H, Harada N, et al. Collective review of small carcinomas of the pancreas. *Ann Surg.* 1986;203:77–81.
6. Furukawa H, Okada S, Saisho H, et al. Clinicopathologic features of small pancreatic adenocarcinoma: a collective study. *Cancer.* 1996;78:986–990.
7. Ariyama J, Suyama M, Satoh K, et al. Imaging of small pancreatic ductal adenocarcinoma. *Pancreas.* 1998;16:396–401.
8. Tsunoda T, Yamamoto Y, Kimoto M, et al. Staging and treatment for patients with pancreatic cancer: how small is an early pancreatic cancer? *J Hepatobiliary Pancreat Surg.* 1998;5:128–132.
9. Ishikawa O, Ohigashi H, Imaoka S, et al. Minute carcinoma of the pancreas measuring 1 cm or less in diameter: collective review of Japanese case reports. *Hepato-Gastroenterology.* 1999;46:8–15.
10. Pantalone D, Ragionieri I, Gabriella N. Improved survival in small pancreatic cancer. *Dig Surg.* 2001;18:41–46.
11. Tsuchiya R, Tajima Y, Matsuzaki S, et al. Early pancreatic cancer. *Pancreatology.* 2001;1:597–603.
12. Egawa S, Takeda K, Furukawa S, et al. Clinicopathological aspects of small pancreatic cancer. *Pancreas.* 2004;28:235–240.
13. Shimada K, Sakamoto Y, Sano T, et al. Reappraisal of the clinical significance of tumor size in patients with pancreatic ductal carcinoma. *Pancreas.* 2006;33:233–239.
14. Takagi K, Ikeda S, Nakagawa Y, et al. A study of duodenal fiberscopy (in Japanese with English abstract). *Stomach Intestine.* 1968;3: 1735–1742.
15. Ikeda S. Thirty three year's experiences of ERCP & its related procedures: from the dawning of ERCP to the present day (in Japanese with English abstract). *Gastroenterol Endosc.* 2005;47:1185–1203.
16. Takagi K, Ikeda S, Nakagawa Y, et al. Retrograde pancreatography and cholangiography by fiber duodenoscope. *Gastroenterology.* 1970; 59:445–452.
17. Takagi K, Takahashi T, Hori M, et al. Small carcinoma of head of the pancreas discovered by the clue of transitory elevation of urinary amylase level (in Japanese with English abstract). *Stomach Intestine.* 1980;15:637–640.
18. Furuta K, Watanabe H, Ikeda S. Differences between solid and duct-ectatic type of pancreatic ductal carcinoma. *Cancer.* 1992;69:1327–1333.
19. Ikeda S, Yoshimoto H, Tanaka M. Retrograde cholangiography with an indwelling balloon catheter placed by duodenoscopy and its application to pancreatography (in Japanese with English abstract). *Gastroenterol Endosc.* 1982;24:1563–1569.
20. Ikeda S, Matsumoto S, Yoshimoto H, et al. Endoscopic balloon catheter pancreatography using catheter retaining technique: usefulness of supine spot films by compression for complete evaluation of pancreatic ducts and branches (in Japanese with English abstract). *Stomach Intestine (Tokyo).* 1984;19:1231–1242.
21. Ikeda S, Watanabe H, Furuta K. *Pancreatic Diseases from a Pancreatographic Viewpoint: Clinical and Pathological Evaluation (in Japanese).* Tokyo: Igakushoin; 1991.
22. Maeshiro K, Ikeda S, Yasunami Y, et al. Balloon-catheter endoscopic retrograde pancreatography-compression study for diagnosis of early-stage pancreatitis. *J Gastroenterol.* 2007;42(suppl XVII):95–102.
23. Japan Pancreas Society. *Classification of Pancreatic Cancer, 2nd English ed.* Tokyo: Kanehara; 2003.
24. Yonezawa S, Nakamura A, Horinouchi M, et al. The expression of several types of mucin is related to the biological behavior of pancreatic neoplasms. *J Hepatobiliary Pancreat Surg.* 2002;9:328–341.
25. Chang KJ, Nguyen P, Erickson RA, et al. The clinical utility of endoscopic ultrasound-guided fine-needle aspiration in the diagnosis and staging of pancreatic carcinoma. *Gastrointest Endosc.* 1997;45: 387–393.
26. Maguchi H. The role of endoscopic ultrasonography in the diagnosis of pancreatic tumors. *J Hepatobiliary Pancreat Surg.* 2004;11:1–3.
27. Abe M, Hara Y, Kiyonari H, et al. Early diagnosis of cancer of body of the pancreas (in Japanese). *Jpn J Gastroenterol.* 1981;78:1676.
28. Gullo L, Pezzilli R, Labate AMM, et al. Diabetes and the risk of pancreatic cancer. *N Engl J Med.* 1994;331:81–84.
29. Ogawa Y, Tanaka M, Inoue K, et al. A prospective pancreatographic study of the prevalence of pancreatic carcinoma in patients with diabetes mellitus. *Cancer.* 2002;94:2344–2349.
30. Chari ST, Leibson CL, Rabe KG, et al. Pancreatic cancer-associated diabetes mellitus: Prevalence and temporal association with diagnosis of cancer. *Gastroenterology.* 2008;134:95–101.
31. Pannala R, Leirness JB, Bamlet WR, et al. Prevalence and clinical profile of pancreatic cancer-associated diabetes mellitus. *Gastroenterology.* 2008;134:981–987.
32. Nakaizumi A, Tatsuta M, Uehara H, et al. Usefulness of simple endoscopic aspiration cytology of pancreatic juice for diagnosis of early pancreatic neoplasm: a prospective study. *Dig Dis Sci.* 1997;42: 1796–1803.
33. Shimizu Y, Yasui K, Matsueda K, et al. Small carcinoma of the pancreas is curable: new computed tomography finding, pathological study and postoperative results from a single institute. *J Gastroenterol Hepatol.* 2005;20:1591–1594.
34. Furuta K, Ikeda S, Watanabe H, et al. Branch duct origin of solid type pancreatic ductal carcinoma. *Aust NZ J Surg.* 1993;63:405–409.
35. Takaori K, Matsusue S, Hujikawa T, et al. Carcinoma in situ of the pancreas associated with localized fibrosis: A clue to early detection of neoplastic lesions arising from pancreatic ducts. *Pancreas.* 1998; 17:102–105.
36. Kozuka S, Sassa R, Taki T, et al. Relation of pancreatic duct hyperplasia to carcinoma. *Cancer.* 1979;43:1418–1428.
37. Brat DJ, Lillemoe KD, Yeo CJ, et al. Progression of pancreatic intraductal neoplasias to infiltrating adenocarcinoma of the pancreas. *Am J Surg Pathol.* 1998;22:163–169.

38. Hruban RH, Adsay NV, Albores-Saavedra J, et al. Pancreatic intraepithelial neoplasia: a new nomenclature and classification system for pancreatic duct lesions. *Am J Surg Pathol.* 2000;25: 579–586.

39. Hruban RH, Takaori K, Klimstra DS, et al. An illustrated consensus on the classification of pancreatic intraepithelial neoplasia and intraductal papillary mucinous neoplasms. *Am J Surg Pathol.* 2004; 28:977–987.

40. Takaori K. Dilemma in classification of possible precursors of pancreatic cancer involving the main pancreatic duct: PanIN or IPMN? *J Gastroenterol.* 2003;38:311–313.

41. Akashi R, Kiyozumi T, Tanaka T, et al. Mechanism of pancreatitis caused by ERCP. *Gastrointest Endosc.* 2002;55:50–54.

42. Vege SS, Chari ST, Petersen BT, et al. Endoscopic retrograde cholangiopancreatography-induced severe acute pancreatitis. *Pancreatology.* 2006;6:527–530.

43. Ikeda S, Tanaka M, Yoshimoto H, et al. Improved visualization of intrahepatic bile ducts by endoscopic retrograde balloon catheter cholangiography. *Ann Surg.* 1981;194:171–175.

44. Ikeda S, Yoshimoto H, Tanaka M, et al. Cholangiography of intrahepatic bile ducts in hepatolithiasis by endoscopic placement of an indwelling balloon catheter. *Gastrointest Endosc.* 1985;31:181–187.

45. Yoshimoto H, Ikeda S, Tanaka M, et al. Endoscopic retrograde cholangiography with a balloon catheter: analysis of 100 consecutive cases. *Radiology.* 1986;159:53–58.

46. Sobin LH, Wittekind C, eds. *International Union Against Cancer. TNM Classification of Malignant Tumours.* 6th ed. New York: Wiley-Liss; 2002.

High-mobility group box 1 is involved in the initial events of early loss of transplanted islets in mice

Nobuhide Matsuoka,[1,2] Takeshi Itoh,[1] Hiroshi Watarai,[3] Etsuko Sekine-Kondo,[3] Naoki Nagata,[4] Kohji Okamoto,[4] Toshiyuki Mera,[1,2] Hiroshi Yamamoto,[5] Shingo Yamada,[6] Ikuro Maruyama,[7] Masaru Taniguchi,[3] and Yohichi Yasunami[1]

[1]Department of Regenerative Medicine and Transplantation and [2]Department of Gastrointestinal Surgery, Faculty of Medicine, Fukuoka University, Japan. [3]Laboratory for Immune Regulation, RIKEN Research Center for Allergy and Immunology, Yokohama, Japan. [4]Department of Surgery 1, University of Occupational and Environmental Health, School of Medicine, Kitakyushu, Japan. [5]Department of Biochemistry and Molecular Vascular Biology, Kanazawa University Graduate School of Medical Science, Japan. [6]Shino-Test Co., Sagamihara, Japan. [7]Department of Laboratory and Vascular Medicine, Kagoshima University Graduate School of Medical and Dental Sciences, Japan.

Islet transplantation for the treatment of type 1 diabetes mellitus is limited in its clinical application mainly due to early loss of the transplanted islets, resulting in low transplantation efficiency. NKT cell–dependent IFN-γ production by Gr-1$^+$CD11b$^+$ cells is essential for this loss, but the upstream events in the process remain undetermined. Here, we have demonstrated that high-mobility group box 1 (HMGB1) plays a crucial role in the initial events of early loss of transplanted islets in a mouse model of diabetes. Pancreatic islets contained abundant HMGB1, which was released into the circulation soon after islet transplantation into the liver. Treatment with an HMGB1-specific antibody prevented the early islet graft loss and inhibited IFN-γ production by NKT cells and Gr-1$^+$CD11b$^+$ cells. Moreover, mice lacking either of the known HMGB1 receptors TLR2 or receptor for advanced glycation end products (RAGE), but not the known HMGB1 receptor TLR4, failed to exhibit early islet graft loss. Mechanistically, HMGB1 stimulated hepatic mononuclear cells (MNCs) in vivo and in vitro; in particular, it upregulated CD40 expression and enhanced IL-12 production by DCs, leading to NKT cell activation and subsequent NKT cell–dependent augmented IFN-γ production by Gr-1$^+$CD11b$^+$ cells. Thus, treatment with either IL-12– or CD40L-specific antibody prevented the early islet graft loss. These findings indicate that the HMGB1-mediated pathway eliciting early islet loss is a potential target for intervention to improve the efficiency of islet transplantation.

Introduction

Pancreatic islet transplantation, although an attractive procedure for the treatment of type 1 diabetes mellitus, usually fails to achieve insulin independence of a diabetic recipient from a single donor due to early loss of transplanted islets and therefore requires sequential transplantations of islets with the use of 2–3 donors (1). Thus, the low efficiency of islet transplantation has been a major obstacle facing islet transplantation and hampers its clinical application.

We have previously shown in mice that loss of transplanted islets soon after transplantation is caused by NKT cell–dependent IFN-γ production by Gr-1$^+$CD11b$^+$ cells and is successfully prevented by treatment of NKT cells with repeated stimulation with their synthetic ligand, α-galactosylceramide (α-GalCer), to downregulate IFN-γ production of NKT cells, or by depletion of Gr-1$^+$CD11b$^+$ cells with anti–Gr-1 antibody (2). However, precisely how it is involved in the upstream events in the activation of NKT cells and Gr-1$^+$CD11b$^+$ cells in the early loss of transplanted islets remains to be solved.

High-mobility group box 1 (HMGB1) protein was initially found to be a DNA-binding protein present in almost all eukaryotic cells, where it stabilizes nucleosome formation and acts as a nuclear factor that enhances transcription (3, 4). Recently, HMGB1 has been demonstrated to play crucial roles in response to tissue damage, indicating that HMGB1 is a prototype of the emerging damage-associated molecular pattern molecule (4, 5). HMGB1 is also known to be secreted by activated immune cells, including macrophages (6, 7), DCs (8), and NK cells (9) in response to infection and inflammatory stimuli. Once secreted, HMGB1 induces inflammatory responses by transduction of cellular signals through its receptors, such as TLR2, TLR4 (10–12), and receptor for advanced glycation end products (RAGE) (8, 13, 14). Moreover, HMGB1 levels are markedly increased during severe sepsis in humans and animals, and administration of neutralizing HMGB1-specific antibodies prevents lethality from sepsis (6). Recent accumulating evidence now suggests that HMGB1 acquires or augments proinflammatory activity by binding to proinflammatory mediators such as LPS, IL-1 (14), and DNA (15–17). These observations indicate that HMGB1 is an essential mediator of organ damage; however, its precise role and mechanism remain unknown. Here, we investigate the mechanisms of action of HMGB1 in the early loss of transplanted islets.

Results

Involvement of HMGB1 in early loss of transplanted islets. It has previously been shown that hyperglycemia of streptozotocin-induced (STZ-induced) diabetic recipient mice was ameliorated after transplantation of 400 syngenic islets in the liver but not of 200 islets (Figure 1A, no treatment), the number of islets isolated from a

Authorship note: Nobuhide Matsuoka, Takeshi Itoh, and Hiroshi Watarai contributed equally to this work.

Conflict of interest: The authors have declared that no conflict of interest exists.

Citation for this article: *J Clin Invest* doi:10.1172/JCI41360.

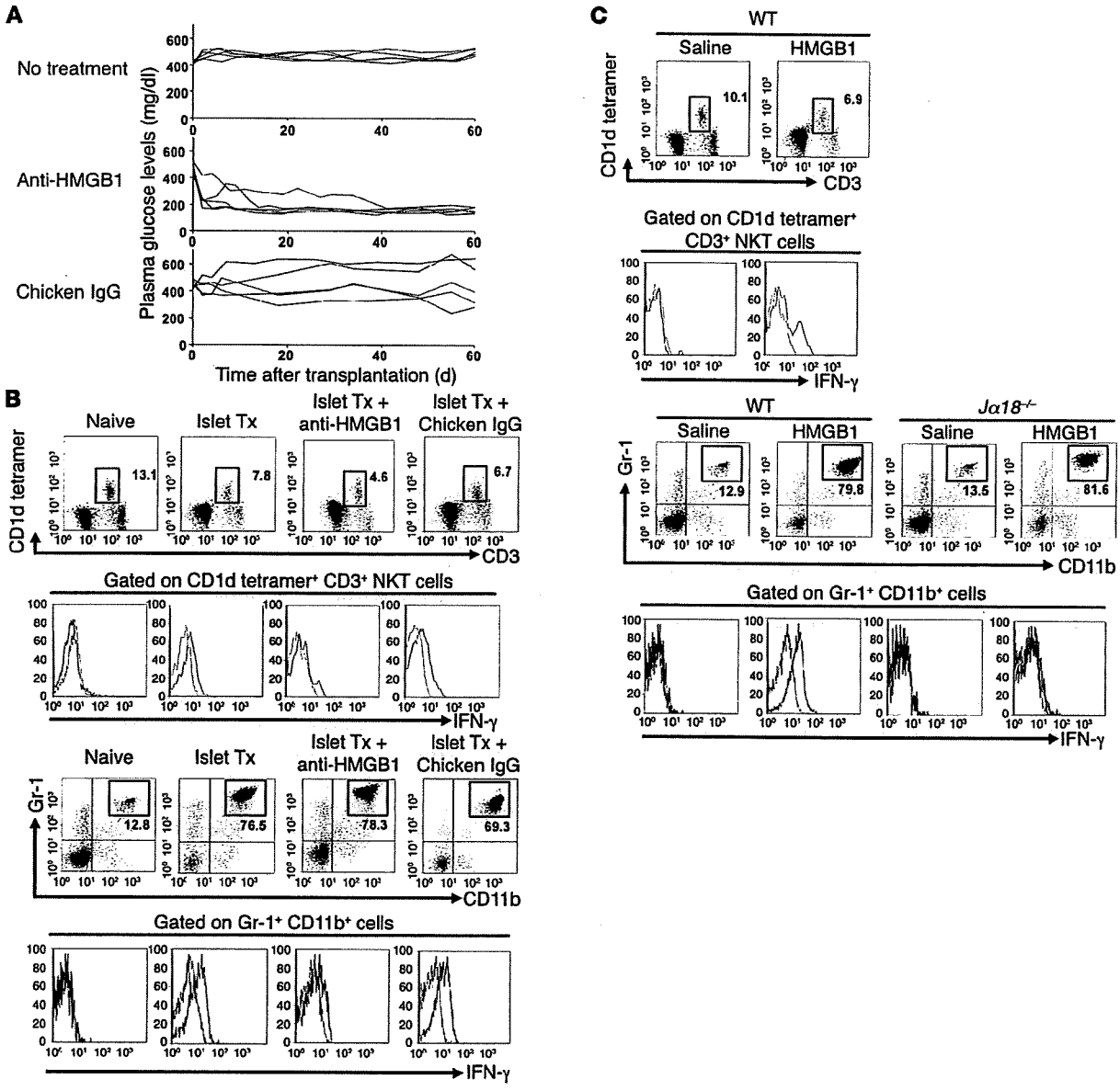

Figure 1

Essential roles of HMGB1 in early loss of transplanted islets. (**A**) Nonfasting plasma glucose levels in STZ-induced diabetic mice received 200 syngeneic islets (top panel) and those treated with chicken anti-HMGB1 antibody or control chicken IgG. Individual lines represent glucose levels of each animal. (**B**) FACS profiles of liver MNCs from naive mice, STZ-induced diabetic mice that received 200 syngenic islets (Islet Tx), and islet transplanted mice treated with anti-HMGB1 antibody or with chicken IgG. NKT cells (top 2 rows) and Gr-1$^+$CD11b$^+$ cells (bottom 2 rows) were analyzed for IFN-γ (second and fourth rows). The numbers in the figures represent the percentage of cells in the corresponding square areas. Representative data from 4 experiments are shown. (**C**) FACS profiles of NKT cells and Gr-1$^+$CD11b$^+$ cells after HMGB1 treatment. Liver MNCs from wild-type or *Jα18*$^{-/-}$ mice treated with i.v. injection of saline or HMGB1 (100 μg/mouse) were isolated 2 hours after the injection and examined by flow cytometry for IFN-γ production by NKT cells and Gr-1$^+$CD11b$^+$ cells. The numbers in the figures represent the percentage of cells in the corresponding square areas. Representative data from 4 experiments are shown.

single mouse pancreas (2). By using the diabetes model mice, we first investigated the effects of anti-HMGB1 antibody to examine whether HMGB1 is directly involved in early loss of transplanted islets. STZ-induced diabetic mice that received 200 islets together with anti-HMGB1 antibody once at the time of islet transplantation became normoglycemic, in contrast to mice treated with control chicken IgG (Figure 1A). The results demonstrated that the anti-HMGB1 antibody ameliorates hyperglycemia of diabetic mice, indicating that the early loss of transplanted islets is prevented by anti-HMGB1. Thus, HMGB1 plays a crucial role in early loss of transplanted islets.

IFN-γ production of NKT cells and Gr-1$^+$CD11b$^+$ cells in the liver receiving islets is inhibited by anti-HMGB1 antibody. Next, we determined whether anti-HMGB1 antibody treatment has any effect on IFN-γ

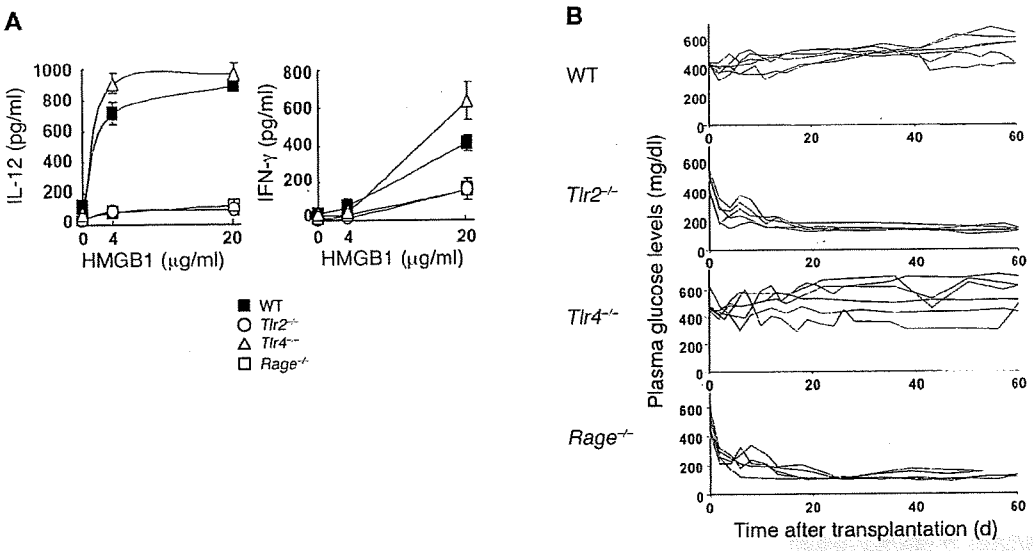

Figure 2
HMGB1 receptors involved in early loss of transplanted islets. (A) In vitro cytokine production by liver MNCs. Liver MNCs (2×10^6/well) isolated from wild-type, *Tlr2*$^{-/-}$, *Tlr4*$^{-/-}$, or *Rage*$^{-/-}$ mice were cultured with indicated doses of HMGB1 in vitro for 48 hours, and IL-12 or IFN-γ levels in the culture supernatant were measured. Representative data from 2 experiments are shown. (B) Nonfasting plasma glucose levels of STZ-induced diabetic wild-type, *Tlr2*$^{-/-}$, *Tlr4*$^{-/-}$, or *Rage*$^{-/-}$ mice that received 200 syngeneic islets. Individual lines represent the glucose level of each animal.

production by NKT cells and Gr-1$^+$CD11b$^+$ cells in the liver of mice receiving islets, which are essential components of early loss of transplanted islets, as shown previously (2). For those purposes, mononuclear cells (MNCs) in the liver of recipient mice were isolated at 6 hours after islet transplantation of 200 syngenic islets into the liver and examined by FACS as to IFN-γ production by NKT cells and Gr-1$^+$CD11b$^+$ cells in the liver. The results are in agreement with the previous findings (2) that, within 6 hours after transplantation of syngeneic islets into the liver, NKT cells and Gr-1$^+$CD11b$^+$ cells accumulated into the liver with upregulated production of IFN-γ (Figure 1B). This upregulated production of IFN-γ after islet transplantation was inhibited by anti-HMGB1. Since the treatment with anti-HMGB1 antibody did not affect the number of infiltrated Gr-1$^+$CD11b$^+$ cells (Figure 1B), the recruitment of Gr-1$^+$CD11b$^+$ cells was due not to HMGB1, but rather probably to the events of transplantation itself. These findings suggest that HMGB1 is essentially involved in the activation of NKT cells and/or Gr-1$^+$CD11b$^+$ cells in the liver after islet transplantation.

NKT cell–dependent IFN-γ production by Gr-1$^+$CD11b$^+$ cells upon stimulation with HMGB1. In order to confirm HMGB1-dependent IFN-γ production, we investigated whether HMGB1 has any stimulatory effects in vivo on NKT cells and/or Gr-1$^+$CD11b$^+$ cells in the liver of mice (Figure 1C). For those purposes, HMGB1 was administered i.v. into naive wild-type and NKT cell–deficient *Jα18*$^{-/-}$ mice, and their hepatic MNCs were isolated at 2 hours after the injection and examined by flow cytometry. It was found that IFN-γ production was upregulated in NKT cells and Gr-1$^+$CD11b$^+$ cells in the liver of wild-type mice treated with HMGB1 (Figure 1C). Importantly, the IFN-γ production by Gr-1$^+$CD11b$^+$ cells in the liver of *Jα18*$^{-/-}$ mice treated with HMGB1 was not upregulated, although accumulation of Gr-1$^+$CD11b$^+$ cells was similar to that in wild-type mice (Figure 1C). These findings indicate that IFN-γ production by Gr-1$^+$CD11b$^+$ cells in the liver of mice treated with HMGB1 is dependent on NKT cells.

Involvement of TLR2 and RAGE but not TLR4 in HMGB1-dependent early loss of transplanted islets. We further investigated whether HMGB1-dependent early loss of transplanted islets is dependent on TLR2, TLR4, and/or RAGE, which is known to be a potential receptor of HMGB1 (10–14). Isolated liver MNCs from wild-type mice induced augmented production of IL-12 and IFN-γ in response to HMGB1 in vitro (Figure 2A), which were greatly reduced in *Tlr2*$^{-/-}$ and *Rage*$^{-/-}$ liver MNCs but not in *Tlr4*$^{-/-}$ liver MNCs, whose cytokine production levels were equivalent to those of wild-type mice in response to HMGB1.

To elucidate which receptor(s) for HMGB1 are actually involved in early loss of transplanted islets, STZ-induced diabetic *Tlr2*$^{-/-}$, *Tlr4*$^{-/-}$, or *Rage*$^{-/-}$ mice that received 200 syngenic islets were investigated for glucose levels in the serum. Interestingly, all of *Tlr2*$^{-/-}$ or *Rage*$^{-/-}$ mice (5 of 5) became normoglycemic, while *Tlr4*$^{-/-}$ mice remained hyperglycemic after transplantation, indicating that TLR2 and RAGE, but not TLR4, play an essential role in the early loss of transplanted islets (Figure 2B).

Pancreatic islet cells are a major source of HMGB1, which mediates IFN-γ production by NKT cells and Gr-1$^+$CD11b$^+$ cells. To validate the involvement of HMGB1 in early loss of transplanted islets, we carried out histological examination on islets before and after transplantation. HMGB1 was detected at a high level in cytoplasm as well as nucleus of transplanted islets as early as 3 hours after transplantation, while HMGB1 was stained only in the nucleus of islets in the naive pancreas and of isolated islets (Figure 3A). The results suggest that HMGB1 is localized in the nucleus of pancreatic islets, shuttled to cytoplasm, and possibly secreted into the circulation soon after transplantation.

Next, we examined the amounts of HMGB1 in isolated islets in comparison with those in other organs, including the thymus, lung, spleen, liver, and pancreas, as well as of FACS-sorted liver MNCs, including NK, NKT, T, B, Gr-1$^-$CD11b$^+$, and Gr-1$^+$CD11b$^+$ cells. Currently, there are no data available with respect to the HMGB1 content in the different cell types, although tissue dis-

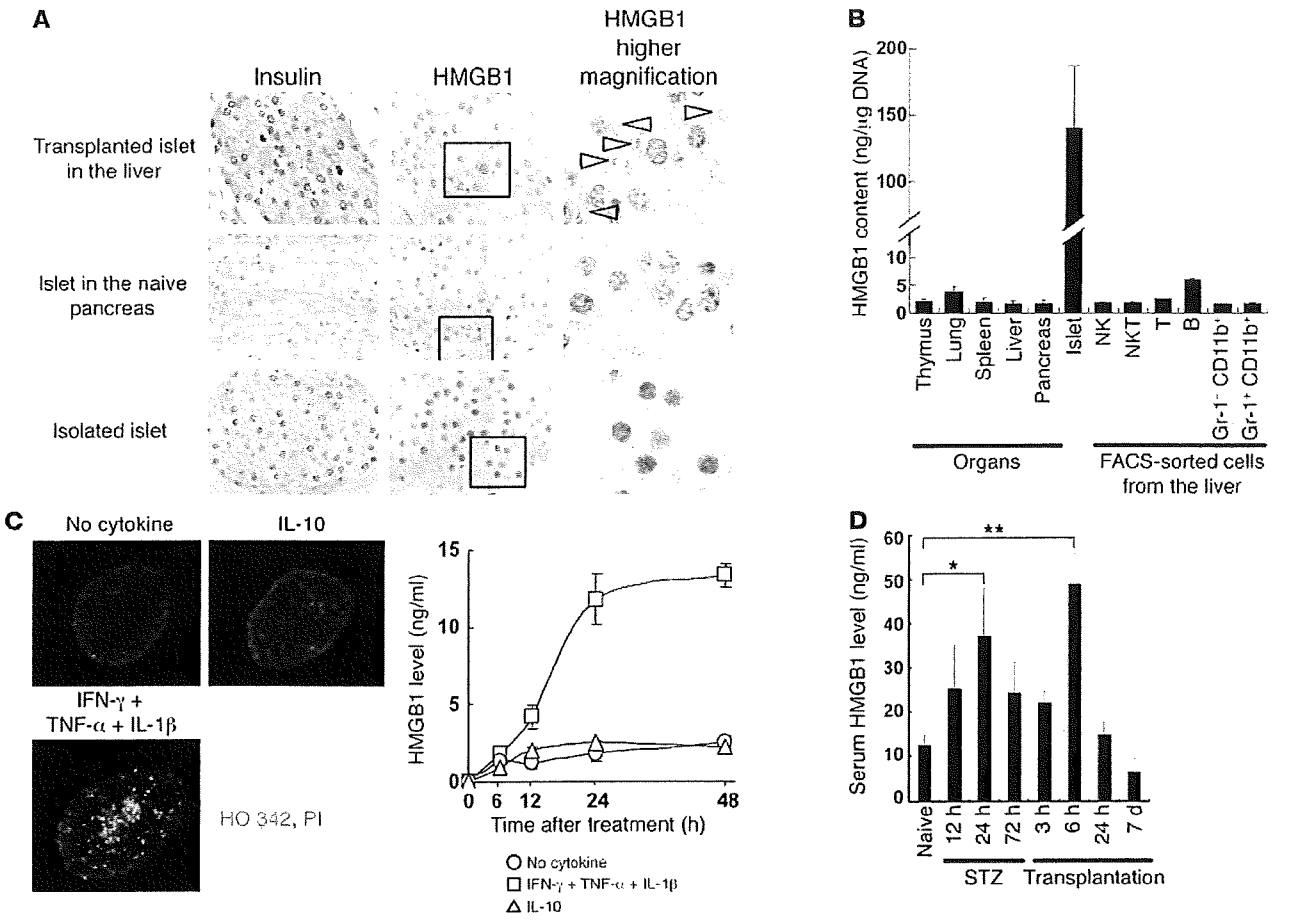

Figure 3

HMGB1 production in tissues and cell types. (**A**) Photomicrographs of islets. Islet cells 3 hours after transplantation in the liver (top row) and those of naive pancreas or isolated islets were examined. Sections stained with anti-insulin or anti-HMGB1 followed by staining with hematoxylin are shown. In general, HMGB1 was detected in the nucleus (brown), while some was detected in cytoplasm, as indicated by arrowheads. Original magnification: ×100 (first and second columns) and ×800 (third column). Boxed regions in the second column were enlarged. (**B**) HMGB1 contents (ng/μg DNA) of individual organs (n = 5), isolated islets, or FACS-sorted liver MNCs (n = 3). (**C**) Left panels: Fluorescence photomicrographs of isolated islets (original magnification, ×200) stained with HO 342 (blue) and PI (red) at 24 hours after in vitro culture with or without IFN-γ, TNF-α, and IL-1β (20 ng/ml each) or IL-10 (20 ng/ml). Right panels: HMGB1 levels in the culture (200 cells/dish) were also measured at the indicated time points in the absence of cytokine or the presence of cytokine mixtures or of control cytokine (IL-10). The values are expressed as the mean ± SD in each group (n = 5). (**D**) Serum HMGB1 levels were measured after STZ injection and also after transplantation of 400 syngeneic islets, which had been performed 72 hours after STZ injection (n = 5–6). The values are expressed as the mean ± SD. $^*P < 0.05$; $^{**}P < 0.01$.

tribution of HMGB1 has been reported previously (18). To our surprise, isolated islets contained high levels of HMGB1, which were 20 times more greater than in other organs or FACS-sorted cells tested (Figure 3B). The physiological roles of high concentrations of HMGB1 in islet cells as well as their etiology are a matter of interest and need to be clarified in future studies.

To investigate a direct relationship between HMGB1 and islet cell damage, we cultured isolated mouse islets in the absence or presence of cytotoxic proinflammatory cytokines, including IFN-γ, TNF-α, and IL-1β, which are known to induce islet cell death in vitro (19) with elevated concentrations of HMGB1 in the culture medium (20). IL-10 was used as a control. Islet cell death was assessed by fluorescence microscopy with the use of the DNA-binding dye propidium iodide (PI) and Hoechst 33342 (HO 342) (19). PI, a highly polar dye that is impermeable to cells with preserved membranes, stains DNA red when membranes are damaged. HO 342 freely passes the plasma membrane, readily enters cells with intact membranes, and stains DNA blue. Thus, the nuclei of dead cells stained red by PI, while those of intact cells stained blue without fragmentation and condensation by HO 342. PI-positive islet cells were increased in number with time in the presence of cytotoxic cytokines, while those in the absence of cytotoxic cytokines and in the presence of the control cytokine remained low in number (Figure 3C). In parallel, HMGB1 concentration in the islet cell culture medium increased with time in the presence of cytotoxic cytokines, while, in contrast, that in the absence of cytotoxic cytokines as well as in the presence of the control cytokine remained low (Figure 3C).

The above findings suggest that HMGB1 of transplanted islets may be released into the circulation of recipient mice in association with their damage soon after transplantation. In fact, the serum

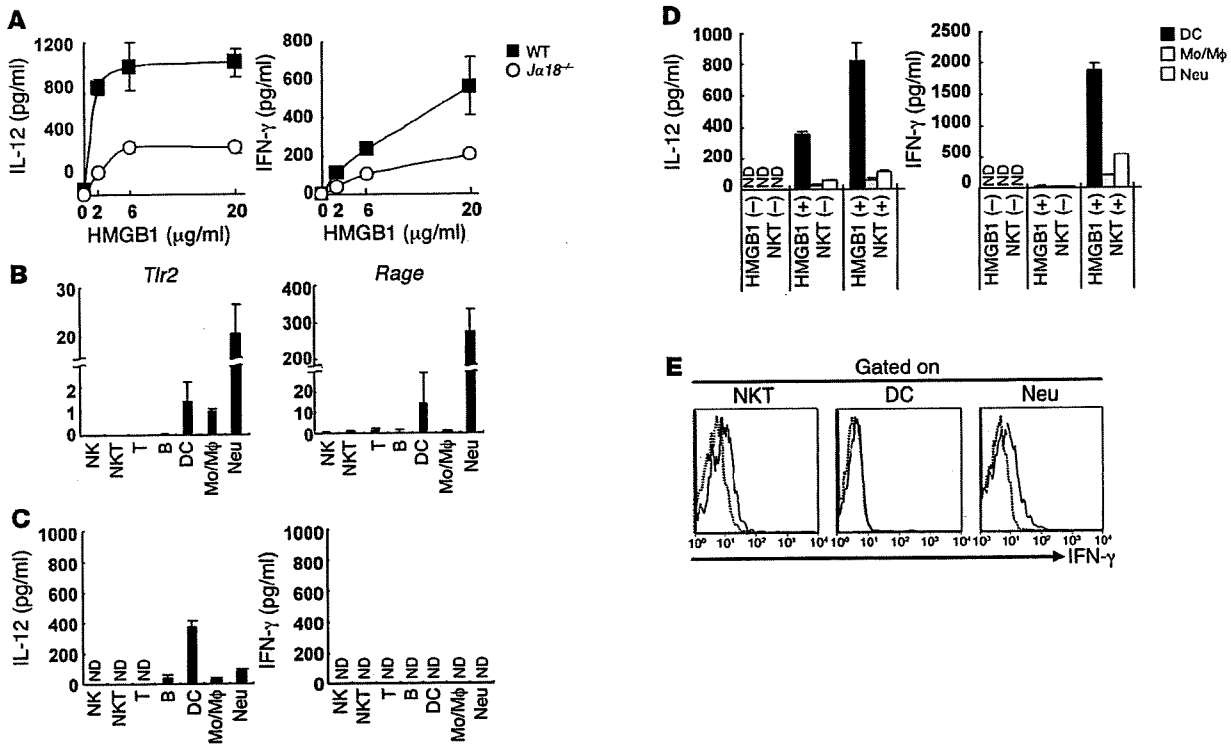

Figure 4

NKT cell–dependent IL-12 and IFN-γ production by liver MNCs in response to HMGB1. (**A**) Liver MNCs (2 × 10^6/well) isolated from wild-type or *Jα18*$^{-/-}$ mice were cultured with the indicated doses of HMGB1 in vitro for 48 hours and measured for IL-12 and IFN-γ. Representative data from 2 experiments are shown. (**B**) PCR analysis on HMGB1 receptors. FACS-sorted liver MNCs (2 × 10^3 for *Tlr2*, *Rage*, or *Hprt*) were analyzed for mRNA levels by quantitative real-time PCR. Data were analyzed by the ΔΔCt method using the expression level in Mo/Mφ as normalized control. (**C**) Cytokine production in FACS-sorted liver MNCs upon stimulation with HMGB1. FACS-sorted cells were cultured in vitro (1 × 10^5 cells/well) for 48 hours in the presence of HMGB1 (20 μg/ml). The amounts of IL-12 and IFN-γ were measured by CBA (n = 3). (**D**) Cytokine production by DCs, Mo/Mφ, or Neu in the presence of NKT cells. FACS-sorted Gr-1$^-$CD11b$^+$CD11c$^+$ DCs, Gr-1$^-$CD11b$^+$CD11c$^-$ Mo/Mφ, and Gr-1$^+$CD11b$^+$CD11c$^-$ Neu (4 × 10^4) were cocultured in vitro with NKT cells (2 × 10^5) in the presence of HMGB1 (20 μg/ml) for 48 hours. The amounts of IL-12 and IFN-γ were measured by CBA (n = 3). (**E**) Intracellular cytokine staining of liver MNCs after HMGB1 treatment. Liver MNCs (2 × 10^6) were cultured with HMGB1 (20 μg/ml) for 24 hours, and the indicated cells were gated and analyzed for their production of IFN-γ by intracellular cytokine staining.

HMGB1 levels in the STZ-induced diabetic mice were elevated, with a peak at 24 hours, and returned to the preinjection levels by 72 hours after i.v. injection of STZ, while, after islet transplantation, HMGB1 peaked at 6 hours and returned to pretransplant levels by 7 days (Figure 3D). The findings suggest that the first peak of the serum HMGB1 elevation is due to islet cell damage caused by STZ injection, which is a toxic agent to β cells of islets, while the second HMGB1 peak is due to the early loss of transplanted islets.

Cell types responsible for HMGB1-mediated cytokine production. We investigated the mechanisms of action of HMGB1 by measuring in vitro production of IFN-γ and IL-12 in the culture of isolated liver MNCs from wild-type and *Jα18*$^{-/-}$ mice in response to HMGB1, since IFN-γ is critical in the early islet graft loss (2) and also because IL-12 is essential for IFN-γ production by NKT cells (21). Isolated liver MNCs from wild-type mice induced augmented production of IL-12 and IFN-γ in response to HMGB1 in vitro (Figure 4A). Importantly, the amount of IL-12 and IFN-γ produced by liver MNCs in NKT cell-deficient *Jα18*$^{-/-}$ mice treated with HMGB1 was greatly reduced (Figure 4A), indicating that NKT cells augment HMGB1-dependent IL-12 and IFN-γ production.

We then investigated expression of *Tlr2* and *Rage* by quantitative real-time PCR in each FACS-sorted cellular population from the liver, including NK1.1$^+$CD3$^-$ NK, α-GalCer/CD1d dimer$^+$ NKT, CD3$^+$ T, and CD19$^+$ B cells; Gr-1$^+$CD11b$^+$CD11c$^-$ neutrophils (Neu); and Gr-1$^-$CD11b$^+$ cells, which were further divided into CD11c$^+$F4/80$^-$ DCs and CD11c$^-$F4/80$^+$ monocytes/macrophages (Mo/Mφ) (Supplemental Figure 1; supplemental material available online with this article; doi:10.1172/JCI41360DS1). *Tlr2* and *Rage* were detected at high levels on Neu (Figure 4B). DCs also expressed modest levels of both *Tlr2* and *Rage*. However, Mo/Mφ expressed modest levels of *Tlr2* but low levels of *Rage*, while expression of either *Tlr2* or *Rage* was barely detected in other cell populations (NK, NKT, T, and B cells) (Figure 4B).

In order to dissect further the mechanisms of action of HMGB1, we investigated in vitro IL-12 and IFN-γ production in the culture of FACS-sorted individual cellular populations from liver MNCs in response to HMGB1. IL-12 was mainly produced from DCs rather than Neu or Mo/Mφ (Figure 4C). However, IFN-γ production was not detected in any individual cell population among all liver MNC subpopulations tested (Figure 4C).

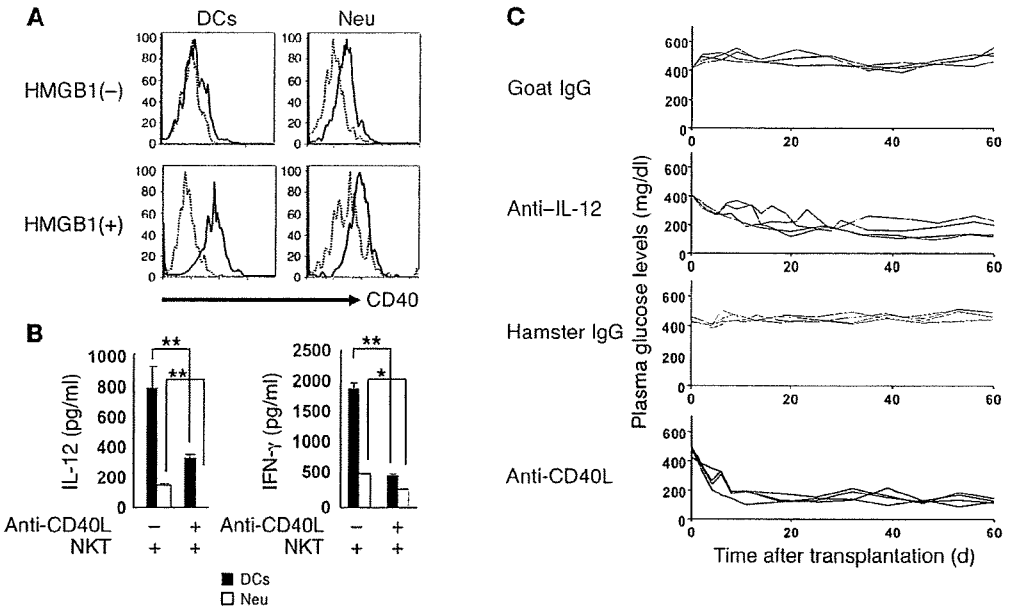

Figure 5

Involvement of CD40-CD40L interaction in production of IL-12 and IFN-γ in early loss of transplanted islets. (**A**) CD40 expression in DCs and Neu before or after treatment with HMGB1. Liver MNCs (2×10^6) were treated without or with HMGB1 (20 μg/ml) for 24 hours and analyzed for CD40 expression ($n = 3$). (**B**) Requirement of CD40-CD40L interaction in the production of IL-12 and IFN-γ in the presence of NKT cells. DCs or Neu (4×10^4) were cocultured in vitro with NKT cells (2×10^5) in the presence of HMGB1 (20 μg/ml) for 48 hours with or without addition of anti-CD40L antibody. IL-12 and IFN-γ levels were measured by CBA ($n = 3$). The values are expressed as the mean ± SD. $^*P < 0.05$; $^{**}P < 0.01$. (**C**) Nonfasting plasma glucose levels of STZ-induced diabetic mice that had received 200 syngeneic islets and were treated with control goat IgG or goat anti-mouse IL-12 antibody and those with control hamster IgG or hamster anti-mouse CD40L antibody with 200 μg intraperitoneal injection per mouse at the time of transplantation. Individual lines represent the nonfasting plasma glucose levels of each diabetic mouse after islet transplantation.

Since IL-12 was produced in vitro from DCs in response to HMGB1 (Figure 4C) and since NKT cell-dependent IFN-γ production by Neu is an essential component of early loss of transplanted islets as shown previously (2), IL-12 and IFN-γ production of FACS-sorted DCs, Mo/Mϕ, or Neu cocultured in the presence of NKT cells with addition of HMGB1 was examined. The production of IL-12 was greatly augmented in response to HMGB1, especially when DCs were cocultured with NKT cells (Figure 4D). The production of IFN-γ became evident in the culture medium of DCs cocultured with NKT cells in the presence of HMGB1 (Figure 4D). The cell types responsible for the production of IFN-γ in response to HMGB1 in Figure 4D were NKT cells but not DCs, because intracellular cytokine staining revealed that NKT cells, but not DCs, produced IFN-γ (Figure 4E). It was also shown that Neu production of IFN-γ was augmented in the presence of NKT cells (Figure 4D).

It is known that IFN-γ production by NKT cells is largely dependent on the interaction between CD40L expression on activated NKT cells and CD40 expression on DCs (22). Thus, we measured CD40 expression on DCs and Neu stimulated with HMGB1. CD40 surface expression was detected in both cell types in resting conditions, while upregulation of CD40 was observed in DCs rather than Neu in HMGB1-treated conditions (Figure 5A). Furthermore, production of both IL-12 and IFN-γ mounted in vitro by HMGB1 stimulation was blocked by anti-CD40L antibody (Figure 5B), indicating that augmented IL-12 production from DCs and Neu and also IFN-γ production by NKT cells and Neu are triggered by CD40/CD40L interaction.

To confirm the data shown in Figure 5, A and B, we determined in vivo requirement of IL-12 and CD40-CD40L interaction in early loss of transplanted islets. Hyperglycemia of STZ diabetic mice receiving 200 syngenic islets in the liver was ameliorated by treatment with either anti-IL-12 or anti-CD40L antibody once at the time of islet transplantation, while that of mice treated with control antibody was not (Figure 5C). Together with the previous studies showing that the anti-IFN-γ treatment normalizes hyperglycemia (22), the results indicate that IL-12 and CD40-CD40L interaction together with IFN-γ actually play a crucial role in vivo in early loss of transplanted islets.

Discussion

Among the most important findings of the present study is that pancreatic islets contain abundant HMGB1 compared with other organs and individual cell populations in the liver, the site of islet transplantation. Immunohistochemical staining of the pancreas revealed that HMGB1 is mainly stained in the nucleus of islet cells but not in other cell types, while HMGB1 is detected in the circulation after islet cell damage. In fact, the plasma concentration of HMGB1 in wild-type mice was elevated and peaked at 24 hours after i.v. injection of STZ and returned to the preinjection level 72 hours after STZ injection. The plasma levels of HMGB1 in diabetic recipient mice were elevated after islet transplantation with a peak at 6 hours and returned to pretransplant levels by 24 hours. These findings suggest that the first peak of the elevated HMGB1 levels is caused by destruction of islet cells by a toxic agent of STZ specific to β cells of islets and that the second peak in recipient